

Periodic solutions of coupled Boussinesq equations and Ostrovsky-type models free from zero-mass contradiction

K. R. Khusnutdinova¹ and M. R. Tranter²

¹*Department of Mathematical Sciences, Loughborough University, Loughborough LE11 3TU, UK*

²*Department of Physics and Mathematics, Nottingham Trent University, Nottingham NG11 8NS, UK*

(*Electronic mail: Matt.Tranter@ntu.ac.uk)

(Dated: 1 October 2022)

Coupled Boussinesq equations are used to describe long weakly-nonlinear longitudinal strain waves in a bi-layer with a soft bonding between the layers (e.g. a soft adhesive). From the mathematical viewpoint, a particularly difficult case appears when the linear long-wave speeds in the layers are significantly different (high-contrast case). The traditional derivation of the uni-directional models leads to four uncoupled Ostrovsky equations, for the right- and left-propagating waves in each layer. However, the models impose a “zero-mass constraint” i.e. the initial conditions should necessarily have zero mean, restricting the applicability of that description. Here, we bypass the contradiction in this high-contrast case by constructing the solution for the deviation from the evolving mean value, using asymptotic multiple-scale expansions involving two pairs of fast characteristic variables and two slow-time variables. By construction, the Ostrovsky equations emerging within the scope of this derivation are solved for initial conditions with zero mean while initial conditions for the original system may have non-zero mean values. Asymptotic validity of the solution is carefully examined numerically. We apply the models to the description of counter-propagating waves generated by solitary wave initial conditions, or co-propagating waves generated by cnoidal wave initial conditions, as well as the resulting wave interactions, and contrast with the behaviour of the waves in bi-layers when the linear long-wave speeds in the layers are close (low-contrast case). One local (classical) and two non-local (generalised) conservation laws of the coupled Boussinesq equations for strains are derived and used to control the accuracy of the numerical simulations.

A weakly-nonlinear solution to the coupled Boussinesq equations on a finite interval with periodic boundary conditions is constructed, resolving the zero-mass contradiction. The solution is shown to be asymptotically valid by comparison to direct numerical simulations of the original coupled Boussinesq equations, with the additional control of derived generalised conservation laws. Examples include counter-propagating radiating solitary waves and Ostrovsky-type wave packets when the period of the solution is large compared to the size of a localised initial condition, while decreasing the period of the solution for the localised perturbations and using non-localised initial conditions leads to more complicated scenarios. We observe that, in many cases, the waves appear to interact in a nearly-elastic manner, similarly to that of solitary waves, with small phase shift and amplitude changes compared to the case with no interaction, while in other cases strong interactions lead to formation of new wave structures.

scaled form:

$$u_{tt} - u_{xx} = \varepsilon \left[\frac{1}{2} (u^2)_{xx} + u_{ttxx} - \delta(u - w) \right], \quad (1)$$

$$w_{tt} - c^2 w_{xx} = \varepsilon \left[\frac{\alpha}{2} (w^2)_{xx} + \beta w_{ttxx} + \gamma(u - w) \right]. \quad (2)$$

This system of equations describes long nonlinear longitudinal strain waves in a bi-layer with a soft bonding between the layers, allowing the layers to move relative to each other.¹⁰ In this context, u and w denote longitudinal strains in the layers, α , β , γ , δ are coefficients depending on the mechanical and geometrical properties of a waveguide, c is the ratio of the characteristic linear wave speeds in the layers and ε is a small amplitude parameter. When the layers have similar properties, radiating solitary waves are found to propagate on large periodic domains.¹¹

In all of these contexts, the natural initial conditions have non-zero mean, and the associated uni-directional equations emerging in the construction of weakly-nonlinear solutions are typically solved numerically using pseudo-spectral schemes with periodic boundary conditions. However, recent work has shown that solving such equations on a periodic domain may require careful attention if the initial conditions have non-zero mean and the periodic domain is comparable to the scale of the initial condition.^{12,13} This was investigated for the Boussinesq-Klein-Gordon (BKG) equation, which can be obtained from the cRB equations by taking the limit $\gamma \rightarrow 0$ with $w = 0$. The weakly-nonlinear solution derived via the traditional procedure leads, at leading order, to two uni-directional Ostrovsky equations, originally developed in the context of fluids¹⁴ (see also Ref. 15). The model nec-

I. INTRODUCTION

Korteweg-de Vries and Boussinesq-type equations have been derived to describe long weakly-nonlinear longitudinal strain waves in rod- and bar-like elastic solids.¹⁻⁹ This paper will focus on the system of coupled regularised Boussinesq (cRB) equations, presented here in non-dimensional and

essarily requires that regular solutions have zero mean initial conditions. The existence of such a formal constraint is known as the “zero-mass (or zero mean) contradiction”¹³ since the original problem formulation does not impose this constraint. However, it was shown that the derivation procedure can be modified in order to develop a weakly-nonlinear solution of the BKG equation for a deviation from the evolving non-zero mean.¹³ Earlier results were developed at the level of Fourier expansions in the spatial variable¹² while the procedure suggested in Ref. 13 can be viewed as a nonlinear extension of the d’Alembert solution. The Ostrovsky equations emerging within the scope of this procedure are solved for zero mean initial conditions by construction, and the zero mean contradiction is avoided. We note that additional conservation laws of the “moment” type were constructed for the Ostrovsky equation in Ref. 16 (see also Ref. 17). However, these conservation laws are not applicable in our case since multiplying a periodic function of some variable by powers of that variable takes us outside of the class of periodic functions. Hence, such conservation laws impose no additional constraints in the periodic case under study.

Considering our cRB equations, when the linear characteristic speeds are close, satisfying the relation $c - 1 = \mathcal{O}(\varepsilon)$ (low-contrast case), and the period of the solution is large compared to the scale of a localised initial condition, we find long-living radiating solitary waves.^{10,18,19} When $c - 1 = \mathcal{O}(1)$, we find wave packets governed by the Ostrovsky equations.^{14,18} In this paper we consider the case when $c - 1 = \mathcal{O}(1)$ (high-contrast case), and the period of the solution is comparable with the scale of the localised initial condition, or when the initial condition is not localised at all. Previously, a simpler case when $c - 1 = \mathcal{O}(\varepsilon)$ was investigated in Ref. 20. As we will obtain single or coupled Ostrovsky equations to leading order, depending on the assumption on the characteristic speeds in the layers, we will need to consider how a weakly-nonlinear solution can be constructed that takes account of the zero-mass contradiction.

The paper is organised as follows. In Section II we construct a weakly-nonlinear solution of the Cauchy problem for the cRB equations (1) - (2) in the case $c - 1 = \mathcal{O}(1)$ on a periodic domain, using asymptotic multiple-scale expansions for the deviation from the oscillating mean values. We use two sets of fast characteristic variables and two slow time variables. The validity of the solutions is examined in Section III by comparing the constructed weakly-nonlinear solution with direct numerical simulations. In Section IV we use both direct numerical simulations and the constructed weakly-nonlinear solutions to study the interaction of counter-propagating waves generated by solitary wave initial conditions, or co-propagating waves generated by cnoidal wave initial conditions, when the characteristic speeds are either close or significantly different. We only consider co-propagating waves for cnoidal wave initial conditions, as this case provides a venue for the study of the strong wave interactions. We also determine the nature of the interaction. In Section V we discuss the local and non-local conservation laws used to control the accuracy of numerical simulations and we conclude our studies in Section VI. The numerical schemes used

in our numerical simulations are described in Supplementary Materials.

II. WEAKLY NONLINEAR SOLUTION

We solve the equation system (1) - (2) on the periodic domain $x \in [-L, L]$. The initial-value (Cauchy) problem is considered, and the initial conditions are written as

$$u(x, 0) = F_1(x), \quad u_t(x, 0) = V_1(x), \quad (3)$$

$$w(x, 0) = F_2(x), \quad w_t(x, 0) = V_2(x). \quad (4)$$

Firstly, we integrate (1) - (2) in x over the period $2L$ to obtain evolution equations of the form

$$\frac{d^2}{dt^2} \int_{-L}^L u(x, t) dx + \varepsilon \delta \int_{-L}^L (u(x, t) - w(x, t)) dx = 0, \quad (5)$$

$$\frac{d^2}{dt^2} \int_{-L}^L w(x, t) dx - \varepsilon \gamma \int_{-L}^L (u(x, t) - w(x, t)) dx = 0. \quad (6)$$

Denoting the mean value of u and w as

$$\langle u \rangle(t) := \frac{1}{2L} \int_{-L}^L u(x, t) dx, \quad \langle w \rangle(t) := \frac{1}{2L} \int_{-L}^L w(x, t) dx, \quad (7)$$

we can solve (5) - (6) to obtain

$$\langle u \rangle = d_1 + \delta d_2 \cos \omega t + d_3 t + \delta d_4 \sin \omega t, \quad (8)$$

$$\langle w \rangle = d_1 - \gamma d_2 \cos \omega t + d_3 t - \gamma d_4 \sin \omega t, \quad (9)$$

where $\omega = \sqrt{\varepsilon(\delta + \gamma)}$. Using the initial conditions (3) - (4) we can determine the values of the coefficients as

$$d_1 = \frac{\gamma \langle F_1 \rangle + \delta \langle F_2 \rangle}{\delta + \gamma}, \quad d_2 = \frac{\langle F_1 \rangle - \langle F_2 \rangle}{\delta + \gamma},$$

$$d_3 = \frac{\gamma \langle V_1 \rangle + \delta \langle V_2 \rangle}{\omega(\delta + \gamma)}, \quad d_4 = \frac{\langle V_1 \rangle - \langle V_2 \rangle}{\omega(\delta + \gamma)}, \quad (10)$$

and we have

$$\langle F_i \rangle = \int_{-L}^L F_i(x) dx, \quad \langle V_i \rangle = \int_{-L}^L V_i(x) dx, \quad i = 1, 2. \quad (11)$$

To simplify the problem we will consider initial conditions that satisfy the condition $d_3 = d_4 = 0$, that is

$$\frac{1}{2L} \int_{-L}^L V_i dx = 0, \quad i = 1, 2. \quad (12)$$

This condition appears naturally in many physical applications and is imposed here to simplify our derivations, however, as was shown for the BKG equation, it can be relaxed (see the Appendix in Ref. 13).

We subtract (8) from u and (9) from w to construct an equation with zero mean value, so we introduce $\tilde{u} = u - \langle u \rangle$ and $\tilde{w} = w - \langle w \rangle$ to obtain the problem for deviations

$$\tilde{u}_{tt} - \tilde{u}_{xx} = \varepsilon \left[\frac{1}{2} (\tilde{u}^2)_{xx} + \langle u \rangle \tilde{u}_{xx} + \tilde{u}_{ttx} - \delta (\tilde{u} - \tilde{w}) \right], \quad (13)$$

$$\tilde{w}_{tt} - c^2 \tilde{w}_{xx} = \varepsilon \left[\frac{\alpha}{2} (\tilde{w}^2)_{xx} + \alpha \langle w \rangle \tilde{w}_{xx} + \beta \tilde{w}_{ttx} + \gamma (\tilde{u} - \tilde{w}) \right], \quad (14)$$

where the expression for $\langle u \rangle$ and $\langle w \rangle$ can be found in (8) and (9) respectively. Note that this problem has variable coefficients, and the traditional procedure used to derive unidirectional models of the Korteweg-de Vries/Ostrovsky type is no longer applicable. The initial conditions become

$$\tilde{u}(x, 0) = \tilde{F}_1(x) = F_1(x) - \langle u \rangle, \quad \tilde{u}_t(x, 0) = V_1(x), \quad (15)$$

$$\tilde{w}(x, 0) = \tilde{F}_2(x) = F_2(x) - \langle w \rangle, \quad \tilde{w}_t(x, 0) = V_2(x), \quad (16)$$

$$u(x, t) = f_1^-(\xi_-, \tau, T) + f_1^+(\xi_+, \tau, T) + \sqrt{\varepsilon} P_1(\xi_-, \xi_+, \tau, T) + \varepsilon Q_1(\xi_-, \xi_+, \tau, T) + \varepsilon^{\frac{3}{2}} R_1(\xi_-, \xi_+, \tau, T) + \varepsilon^2 S_1(\xi_-, \xi_+, \tau, T) + O(\varepsilon^{\frac{5}{2}}), \quad (17)$$

$$w(x, t) = f_2^-(v_-, \tau, T) + f_2^+(v_+, \tau, T) + \sqrt{\varepsilon} P_2(v_-, v_+, \tau, T) + \varepsilon Q_2(v_-, v_+, \tau, T) + \varepsilon^{\frac{3}{2}} R_2(v_-, v_+, \tau, T) + \varepsilon^2 S_2(v_-, v_+, \tau, T) + O(\varepsilon^{\frac{5}{2}}), \quad (18)$$

where we use the characteristic and slow time variables

$$\xi_{\pm} = x \pm t, \quad v_{\pm} = x \pm ct, \quad \tau = \sqrt{\varepsilon} t, \quad T = \varepsilon t.$$

Note that the second time scale, τ , arises from the terms $\langle u \rangle$ and $\langle w \rangle$ as we have the function $\cos(\omega t)$. We can extract the factor of $\sqrt{\varepsilon}$ from ω and write $\cos(\tilde{\omega} \tau)$, where $\tilde{\omega} = \sqrt{\delta + \gamma}$.

As we are considering the solution on the periodic domain, u and w are $2L$ -periodic functions in x . Therefore we require that f_1^- and f_1^+ are periodic in ξ_- and ξ_+ respectively, and similarly f_2^- and f_2^+ are periodic in v_- and v_+ respectively. We then ensure that all functions in the constructed expansion are periodic as well. We will also construct our solution so that functions at each order have zero mean. In particular,

$$\frac{1}{2L} \int_{-L}^L f_1^{\pm} d\xi_{\pm} = 0, \quad \frac{1}{2L} \int_{-L}^L f_2^{\pm} dv_{\pm} = 0. \quad (19)$$

To do this, for the functions in the expansion we will choose appropriate initial conditions, using those found earlier for the cRB equations, so that the initial conditions have zero mean. Where an integration occurs, we will choose any integration constants as the subtraction of the mean value of the function, to enforce zero mean conditions. This will be explained at each step where it occurs. This is consistent with the approach taken in Ref. 13 where we worked in the space of functions with zero mean. In our previous work the integration constants were not explicitly stated in the derivation, but they were implemented to maintain zero mean conditions in the comparisons with the numerical solutions.

As mentioned earlier, the case when $c - 1 = O(\varepsilon)$ was considered in Ref. 20 and the expansions were in the same set of characteristic variables, while here we have two sets of characteristic variables. This means that, at some stage in our derivation, we may encounter a situation where we have a function of v_{\pm} in the equation where the natural set of characteristic variables is ξ_{\pm} . In this case, we can rewrite one set

and, by construction, have zero mean value. The case of $c - 1 = O(\varepsilon)$ was considered in Ref. 20 and so we will only present the derivation for $c - 1 = O(1)$. We will compare the cases in the results section using the derivation in Ref. 20.

In the case when $c - 1 = O(1)$ the characteristic variables cannot be the same in each layer, and instead we have two distinct pairs of characteristic variables. In what follows we omit tildes and look for a weakly-nonlinear solution of the initial-value problem (13) - (16) of the form

of characteristic variables as a linear combination of the other set, so v_{\pm} in terms of ξ_{\pm} , and then proceed. In each case, we will be looking at functions that are fully defined at an earlier order, but are being evaluated in terms of different characteristic variables. A similar situation was encountered in Ref. 18 for the problem considered on the infinite domain, and we will introduce the linear combination when it is required.

We substitute (17) and (18) into (13) and (14), then compare at increasing powers of $\sqrt{\varepsilon}$. The equations are satisfied at leading order so we move onto terms at $O(\sqrt{\varepsilon})$. At this order we have

$$-4P_{1\xi_-\xi_+} - 2f_{1\xi_-\tau}^- + 2f_{1\xi_+\tau}^+ = 0. \quad (20)$$

We average (20) with respect to the fast spatial variable x at constant ξ_- and ξ_+ (see Ref. 13). Averaging $P_{1\xi_-\xi_+}$ at constant ξ_- gives

$$\begin{aligned} \frac{1}{2L} \int_{-L}^L P_{1\xi_-\xi_+} dx &= \frac{1}{4L} \int_{-2L-\xi_-}^{2L-\xi_-} P_{1\xi_-\xi_+} d\xi_+ \\ &= \frac{1}{4L} [P_{1\xi_-}]_{-2L-\xi_-}^{2L-\xi_-} = 0, \end{aligned} \quad (21)$$

with a similar result for averaging at constant ξ_+ . Applying the averaging to (20) and requiring that f_1^{\pm} have zero mean, we find

$$\begin{aligned} f_{1\xi_-\tau}^- = 0 &\implies f_1^- = f_1^-(\xi_-, T), \\ f_{1\xi_+\tau}^+ = 0 &\implies f_1^+ = f_1^+(\xi_+, T). \end{aligned} \quad (22)$$

A similar approach for the equation in w gives

$$f_2^- = f_2^-(v_-, T) \quad \text{and} \quad f_2^+ = f_2^+(v_+, T). \quad (23)$$

Substituting (22) into (20) we obtain

$$P_{1\xi_-\xi_+} = 0 \implies P_1 = g_1^-(\xi_-, \tau, T) + g_1^+(\xi_+, \tau, T), \quad (24)$$

and similarly for w we obtain

$$P_2 = g_2^-(v_-, \tau, T) + g_2^+(v_+, \tau, T). \quad (25)$$

The initial conditions for $f_{1,2}^\pm$ are found by substituting (17) into (3), and also (18) into (4), then comparing terms at $O(1)$, to obtain

$$f_1^\pm|_{T=0} = \frac{1}{2} \left(F_1(\xi_\pm) \pm \left(\int_{-L}^{\xi_\pm} V_1(\sigma) d\sigma - \tilde{V}_1^\pm \right) \right), \quad (26)$$

$$f_2^\pm|_{T=0} = \frac{1}{2c} \left(cF_2(v_\pm) \pm \left(\int_{-L}^{v_\pm} V_2(\sigma) d\sigma - \tilde{V}_2^\pm \right) \right). \quad (27)$$

The values \tilde{V}_1^\pm and \tilde{V}_2^\pm are chosen in such a way to ensure that the initial conditions have zero mean. Explicitly, we calculate \tilde{V}_1^\pm and \tilde{V}_2^\pm as

$$\tilde{V}_1^\pm = \int_{-L}^L \int_{-L}^{\xi_\pm} V_1(\sigma) d\sigma d\xi_\pm, \quad \tilde{V}_2^\pm = \int_{-L}^L \int_{-L}^{v_\pm} V_2(\sigma) d\sigma dv_\pm.$$

This approach of enforcing zero mean will be used at various stages throughout our derivation. To find equations for f_1^\pm and f_2^\pm , we next compare terms at $O(\epsilon)$, using the results from the previous order. Therefore, we find

$$\begin{aligned} -4Q_{1\xi_-\xi_+} = & \left(2f_{1T}^- + f_1^- f_{1\xi_-}^- + d_1 f_{1\xi_-}^- + f_{1\xi_-\xi_-\xi_-}^- \right)_{\xi_-} - \delta(f_1^- - f_2^-) + \left(-2f_{1T}^+ + f_1^+ f_{1\xi_+}^+ + d_1 f_{1\xi_+}^+ + f_{1\xi_+\xi_+\xi_+}^+ \right)_{\xi_+} \\ & - \delta(f_1^+ - f_2^+) + 2g_{1\xi_-\tau}^- - 2g_{1\xi_+\tau}^+ + d_2 \delta \cos(\tilde{\omega}\tau) \left(f_{1\xi_-\xi_-}^- + f_{1\xi_+\xi_+}^+ \right) + f_{1\xi_-\xi_-}^- f_1^+ + 2f_{1\xi_-\xi_-}^- f_{1\xi_+}^+ + f_1^- f_{1\xi_+\xi_+}^+, \end{aligned} \quad (28)$$

$$\begin{aligned} -4c^2 Q_{2v_-v_+} = & \left(2cf_{2T}^- + \alpha f_2^- f_{2v_-}^- + \alpha d_1 f_{2v_-}^- + \beta c^2 f_{2v_-v_-v_-}^- \right)_{v_-} + \gamma(f_1^- - f_2^-) \\ & + \left(-2cf_{2T}^+ + \alpha f_2^+ f_{2v_+}^+ + \alpha d_1 f_{2v_+}^+ + \beta c^2 f_{2v_+v_+v_+}^+ \right)_{v_+} + \gamma(f_1^+ - f_2^+) \\ & + 2cg_{2v_-\tau}^- - 2cg_{2v_+\tau}^+ - \alpha d_2 \gamma \cos(\tilde{\omega}\tau) \left(f_{2v_-v_-}^- + f_{2v_+v_+}^+ \right) + \alpha \left(f_{2v_-v_-}^- f_2^+ + 2f_{2v_-}^- f_{2v_+}^+ + f_2^- f_{2v_+v_+}^+ \right). \end{aligned} \quad (29)$$

Averaging (28) at constant ξ_- or constant ξ_+ gives

$$\pm 2g_{1\xi_\pm\tau} = d_2 \delta \cos(\tilde{\omega}\tau) f_{1\xi_\pm\xi_\pm}^\pm + A_1(\xi_\pm, T), \quad (30)$$

where

$$A_1 = \left(\mp 2f_{1T}^\pm + f_1^\pm f_{1\xi_\pm}^\pm + d_1 f_{1\xi_\pm}^\pm + f_{1\xi_\pm\xi_\pm\xi_\pm}^\pm \right)_{\xi_\pm} - \delta f_1^\pm. \quad (31)$$

To avoid secular terms we require that $A_1 = 0$. Therefore we obtain an Ostrovsky equation for f_1^\pm of the form

$$\left(\mp 2f_{1T}^\pm + f_1^\pm f_{1\xi_\pm}^\pm + d_1 f_{1\xi_\pm}^\pm + f_{1\xi_\pm\xi_\pm\xi_\pm}^\pm \right)_{\xi_\pm} = \delta f_1^\pm. \quad (32)$$

The Ostrovsky equation necessarily requires its regular solutions to have zero mean, and therefore as the initial condition also satisfies this condition, the function f_1^\pm has zero mean. A similar approach for w , averaging at constant v_- or constant v_+ , leads to

$$\pm 2cg_{2v_\pm\tau} = -d_2 \gamma \cos(\tilde{\omega}\tau) f_{2v_\pm v_\pm}^\pm + A_2(v_\pm, T), \quad (33)$$

where again requiring $A_2 = 0$ to avoid secular terms gives an Ostrovsky equation for f_2^\pm of the form

$$\left(\mp 2cf_{2T}^\pm + \alpha f_2^\pm f_{2v_\pm}^\pm + \alpha d_1 f_{2v_\pm}^\pm + \beta c^2 f_{2v_\pm v_\pm v_\pm}^\pm \right)_{v_\pm} = \gamma f_2^\pm, \quad (34)$$

and f_2^\pm has zero mean by construction. Integrating (30) we find an equation for g_1^\pm of the form

$$g_1^\pm = \pm \theta_1 f_{1\xi_\pm}^\pm + G_1^\pm(\xi_\pm, T), \quad (35)$$

and similarly for g_2^\pm we can find

$$g_2^\pm = \mp \theta_2 f_{2v_\pm}^\pm + G_2^\pm(v_\pm, T), \quad (36)$$

where G_1^\pm and G_2^\pm are functions to be found, and we introduce

$$\theta_1 = \frac{d_2 \delta}{2\tilde{\omega}} \sin(\tilde{\omega}\tau), \quad \theta_2 = \frac{\alpha d_2 \gamma}{2c\tilde{\omega}} \sin(\tilde{\omega}\tau). \quad (37)$$

As $f_{1,2}^\pm$ are zero-mean, if the functions $G_{1,2}^\pm$ are also zero-mean then so too is $g_{1,2}^\pm$. We will find an equation for $G_{1,2}^\pm$ at the next order. Substituting (32) and (35) into (28) and integrating we obtain

$$\begin{aligned} Q_1 = & h_{1c}^-(\xi_-, \tau, T) + h_{1c}^+(\xi_+, \tau, T) + h_{1c}(\xi_-, \xi_+, T) \\ & + \hat{f}_2^-(v_-, T) + \hat{f}_2^+(v_+, T), \end{aligned} \quad (38)$$

where

$$\begin{aligned} h_{1c} = & -\frac{1}{4} \left(f_{1\xi_-}^- \int_{-L}^{\xi_+} f_1^+(\sigma) d\sigma + 2f_1^- f_1^+ + f_{1\xi_+}^+ \int_{-L}^{\xi_-} f_1^-(\sigma) d\sigma \right) \\ & - \tilde{h}_{1c}, \end{aligned} \quad (39)$$

and \tilde{h}_{1c} is the mean value of the function, so that the function h_{1c} has zero mean. The function $\hat{f}_2^\pm(v_\pm, T)$ is a function of v_\pm , not ξ_\pm , however we can write the characteristic variables v_\pm in terms of ξ_\pm as

$$v_- = \frac{(1+c)\xi_- + (1-c)\xi_+}{2}, \quad v_+ = \frac{(1-c)\xi_- + (1+c)\xi_+}{2}. \quad (40)$$

Therefore, we can rewrite our functions $f_{1,2}^{\pm}$ in terms of the other set of characteristic variables, and so we find $\hat{f}_2^{\pm}(v_{\pm}, T)$ can be written as

$$\hat{f}_2^{\pm} = \frac{\delta}{c^2 - 1} \int_{-L}^{v_{\pm}} \int_{-L}^z f_2^{\pm}(y, T) dy dz - c_{\hat{f}_2}, \quad (41)$$

where $c_{\hat{f}_2}$ is the appropriately chosen integration constant. Similarly, substituting (34) and (36) into (29) and integrating we find

$$Q_2 = h_2^{-}(v_{-}, \tau, T) + h_2^{+}(v_{+}, \tau, T) + h_{2c}(v_{-}, v_{+}, T) + \hat{f}_1^{-}(\xi_{-}, T) + \hat{f}_1^{+}(\xi_{+}, T), \quad (42)$$

where

$$h_{2c} = -\frac{\alpha}{4c^2} \left(f_{2v_{-}}^{-} \int_{-L}^{v_{+}} f_2^{+}(\sigma) d\sigma + 2f_2^{-} f_2^{+} + f_{2v_{+}}^{+} \int_{-L}^{v_{-}} f_2^{-}(\sigma) d\sigma \right) - \tilde{h}_{2c}, \quad (43)$$

and h_{2c} is the appropriately chosen integration constant. Rewriting ξ_{\pm} in terms of v_{\pm} in a similar way to (40), we have

$$\hat{f}_1^{\pm} = -\frac{\gamma}{c^2 - 1} \int_{-L}^{\xi_{\pm}} \int_{-L}^z f_1^{\pm}(y, T) dy dz - c_{\hat{f}_1}, \quad (44)$$

with $c_{\hat{f}_1}$ an appropriately chosen integration constant so that \hat{f}_1^{\pm} has zero mean. As before we find the initial condition for $G_{1,2}^{\pm}$ by substituting (17) and (18) into (3) and (4), comparing terms at $O(\sqrt{\varepsilon})$. Therefore, taking account of the results found for (35) and (36), and noting that $\theta_1|_{T=0} = 0$, we obtain

$$G_1^{\pm}|_{T=0} = 0 \quad \text{and} \quad G_2^{\pm}|_{T=0} = 0. \quad (45)$$

We now aim to find equations for $G_{1,2}^{\pm}$ and $h_{1,2}^{\pm}$ at the next order. Comparing terms at $O(\varepsilon^{3/2})$ in the expansion of (13) and (14), taking account of results at previous orders, we have

$$\begin{aligned} -4R_{1\xi_{-}\xi_{+}} &= \left(2g_{1T}^{-} + (f_1^{-} g_1^{-})_{\xi_{-}} + d_1 g_{1\xi_{-}}^{-} + g_{1\xi_{-}\xi_{-}}^{-} \right)_{\xi_{-}} - \delta (g_1^{-} - g_2^{-}) + \left(-2g_{1T}^{+} + (f_1^{+} g_1^{+})_{\xi_{+}} + d_1 g_{1\xi_{+}}^{+} + g_{1\xi_{+}\xi_{+}}^{+} \right)_{\xi_{+}} \\ &\quad - \delta (g_1^{+} - g_2^{+}) + 2h_{1\xi_{-}\tau}^{-} - 2h_{1\xi_{+}\tau}^{+} - g_{1\tau\tau}^{-} - g_{1\tau\tau}^{+} + d_2 \delta \cos(\tilde{\omega}\tau) \left(g_{1\xi_{-}\xi_{-}}^{-} + g_{1\xi_{+}\xi_{+}}^{+} \right) \\ &\quad + g_{1\xi_{-}\xi_{-}}^{-} f_1^{+} + 2g_{1\xi_{-}}^{-} f_{1\xi_{+}}^{+} + g_{1\xi_{+}\xi_{+}}^{-} f_1^{+} + g_{1\xi_{+}\xi_{+}}^{+} f_1^{-} + 2g_{1\xi_{+}}^{+} f_{1\xi_{-}}^{-} + g_{1\xi_{-}\xi_{-}}^{+} f_1^{-}, \quad (46) \\ -4c^2 R_{2v_{-}v_{+}} &= \left(2cg_{2T}^{-} + \alpha (f_2^{-} g_2^{-})_{v_{-}} + \alpha d_1 g_{2v_{-}}^{-} + \beta c^2 g_{2v_{-}v_{-}}^{-} \right)_{v_{-}} + \gamma (g_1^{-} - g_2^{-}) \\ &\quad + \left(-2cg_{2T}^{+} + \alpha (f_2^{+} g_2^{+})_{v_{+}} + \alpha d_1 g_{2v_{+}}^{+} + \beta c^2 g_{2v_{+}v_{+}}^{+} \right)_{v_{+}} + \gamma (g_1^{+} - g_2^{+}) \\ &\quad + 2ch_{2v_{-}\tau}^{-} - 2ch_{2v_{+}\tau}^{+} - g_{2\tau\tau}^{-} - g_{2\tau\tau}^{+} - \alpha d_2 \gamma \cos(\tilde{\omega}\tau) \left(g_{2v_{-}v_{-}}^{-} + g_{2v_{+}v_{+}}^{+} \right) \\ &\quad + \alpha \left[g_{2v_{-}v_{-}}^{-} f_2^{+} + 2g_{2v_{-}}^{-} f_{2v_{+}}^{+} + g_{2v_{+}v_{+}}^{-} f_2^{+} + g_{2v_{+}v_{+}}^{+} f_2^{-} + 2g_{2v_{+}}^{+} f_{2v_{-}}^{-} + g_{2v_{-}v_{-}}^{+} f_2^{-} \right]. \quad (47) \end{aligned}$$

Substituting (35) into (46) and averaging at constant ξ_{-} or constant ξ_{+} leads to

$$\begin{aligned} \pm 2h_{1\xi_{\pm}\tau}^{\pm} &= \pm \theta_1 \left(\mp 2f_{1T}^{\pm} + f_1^{\pm} f_{1\xi_{\pm}}^{\pm} + d_1 f_{1\xi_{\pm}}^{\pm} + f_{1\xi_{\pm}\xi_{\pm}}^{\pm} \right)_{\xi_{\pm}\xi_{\pm}} \\ &\quad + \left(\mp 2G_{1T}^{\pm} + (f_1^{\pm} G_1^{\pm})_{\xi_{\pm}} + d_1 G_{1\xi_{\pm}}^{\pm} + G_{1\xi_{\pm}\xi_{\pm}}^{\pm} \right)_{\xi_{\pm}} \\ &\quad \mp \theta_1 \delta f_1^{\pm} - \delta G_{1\xi_{\pm}}^{\pm} \pm \theta_1 \tilde{\omega}^2 f_{1\xi_{\pm}}^{\pm} \\ &\quad \pm \theta_1 d_2 \delta \cos(\tilde{\omega}\tau) f_{1\xi_{\pm}\xi_{\pm}}^{\pm}. \quad (48) \end{aligned}$$

If we differentiate (32) with respect to the appropriate characteristic variable, we can eliminate some terms from (48) to obtain an expression for $h_{1\xi_{\pm}\tau}^{\pm}$ of the form

$$2h_{1\xi_{\pm}\tau}^{\pm} = \theta_1 \tilde{\omega}^2 f_{1\xi_{\pm}}^{\pm} + \theta_1 d_2 \delta \cos(\tilde{\omega}\tau) f_{1\xi_{\pm}\xi_{\pm}}^{\pm} + \tilde{G}_1^{\pm}(\xi_{\pm}, T), \quad (49)$$

where

$$\tilde{G}_1^{\pm} = \left(\mp 2G_{1T}^{\pm} + (f_1^{\pm} G_1^{\pm})_{\xi_{\pm}} + d_1 G_{1\xi_{\pm}}^{\pm} + G_{1\xi_{\pm}\xi_{\pm}}^{\pm} \right)_{\xi_{\pm}} - \delta G_1^{\pm}. \quad (50)$$

To avoid secular terms we require that $\tilde{G}_1^{\pm} = 0$ and therefore we have an equation for G_1^{\pm} of the form

$$\left(\mp 2G_{1T}^{\pm} + (f_1^{\pm} G_1^{\pm})_{\xi_{\pm}} + d_1 G_{1\xi_{\pm}}^{\pm} + G_{1\xi_{\pm}\xi_{\pm}}^{\pm} \right)_{\xi_{\pm}} = \delta G_1^{\pm}. \quad (51)$$

Taking account of the initial condition in (45) and the form of (51), we can clearly see that $G_1^{\pm} \equiv 0$ in this derivation and therefore in all subsequent steps we will omit all terms in G_1^{\pm} . Referring back to (35), we now see that g_1^{\pm} has zero mean. Integrating (49) we obtain

$$h_1^{\pm} = -\frac{\tilde{\omega}^2 \rho_1}{2} f_1^{\pm} - \frac{\tilde{\omega}^2 \rho_1^2}{2} f_{1\xi_{\pm}\xi_{\pm}}^{\pm} + \phi_1^{\pm}(\xi_{\pm}, T), \quad (52)$$

where the functions ϕ_1^\pm are to be found at the next order and

$$\rho_1 = \partial_\tau^{-1} \theta_1 = \frac{d_2 \delta}{2\tilde{\omega}^2} \cos(\tilde{\omega}\tau). \quad (53)$$

If the function ϕ_1^\pm is constructed to have zero mean, then so does h_1^\pm . Similarly, from the equation for w , we find

$$\begin{aligned} \pm 2ch_{2\xi_\pm\tau}^\pm &= \mp \theta_2 \tilde{\omega}^2 f_{2v_\pm}^\pm \pm \theta_2 d_2 \gamma \cos(\tilde{\omega}\tau) f_{2v_\pm v_\pm}^\pm \\ &+ \tilde{G}_2^\pm(v_\pm, T), \end{aligned} \quad (54)$$

where

$$\begin{aligned} \tilde{G}_2^\pm(v_\pm, T) &= \mp 2cG_{2Tv_\pm}^\pm + \alpha(f_2^\pm G_2^\pm)_{v_\pm v_\pm} + \alpha d_1 G_{2v_\pm v_\pm}^\pm \\ &+ \beta c^2 G_{2v_\pm v_\pm v_\pm}^\pm - \gamma G_2^\pm. \end{aligned} \quad (55)$$

We require that $\tilde{G}_2^\pm = 0$ and, by the same argument as for G_1^\pm we have $G_2^\pm \equiv 0$ and therefore omit it from all subsequent derivations, meaning g_2^\pm has zero mean. Integrating (54) we obtain

$$h_2^\pm = \frac{\tilde{\omega}^2 \rho_2}{2c} f_2^\pm - \frac{\tilde{\omega}^2 \rho_2^2}{2} f_{2v_\pm v_\pm}^\pm + \phi_2^\pm(v_\pm, T), \quad (56)$$

where again we need to find the function ϕ_2^\pm and

$$\rho_2 = \partial_\tau^{-1} \theta_2 = \frac{\alpha d_2 \gamma}{2\tilde{\omega}^2} \cos(\tilde{\omega}\tau). \quad (57)$$

If the function ϕ_2^\pm is constructed to have zero mean, then so does h_2^\pm . Substituting (52) into (46) and integrating with respect to the appropriate characteristic variables we find

$$\begin{aligned} R_1 &= \psi_1^-(\xi_-, \tau, T) + \psi_1^+(\xi_+, \tau, T) + \psi_{1c}(\xi_-, \xi_+, T) \\ &+ \hat{g}_2^- + \hat{g}_2^+, \end{aligned} \quad (58)$$

where

$$\begin{aligned} \psi_{1c} &= -\frac{\theta_1}{4} \left[f_{1\xi_+\xi_+}^+ \int_{-L}^{\xi_-} f_1^-(\sigma) d\sigma - f_1^+ f_{1\xi_-}^- + f_1^- f_{1\xi_+}^+ \right. \\ &\left. - f_{1\xi_-\xi_-}^- \int_{-L}^{\xi_+} f_1^+(\sigma) d\sigma \right] - c\psi_{1c}, \end{aligned} \quad (59)$$

with appropriate integration constant to maintain zero mean. The terms \hat{g}_2^\pm can be found by replacing f with g in (41). Similarly, substituting (56) into (47) and integrating gives

$$\begin{aligned} R_2 &= \psi_2^-(v_-, \tau, T) + \psi_2^+(v_+, \tau, T) + \psi_{2c}(\xi_-, \xi_+, T) \\ &+ \hat{g}_1^- + \hat{g}_1^+, \end{aligned} \quad (60)$$

where

$$\begin{aligned} \psi_{2c} &= -\frac{\alpha\theta_2}{4c^2} \left[f_{2v_-v_-}^- \int_{-L}^{v_+} f_2^+(\sigma) d\sigma - f_{2v_-}^- f_2^+ + f_2^- f_{2v_+}^+ \right. \\ &\left. - f_{2v_+v_+}^+ \int_{-L}^{v_-} f_2^-(\sigma) d\sigma \right] - c\psi_{2c}, \end{aligned} \quad (61)$$

with appropriate integration constant to maintain zero mean. The expression for \hat{g}_1^\pm can be found by replacing f with g in (44). The exact form of these terms is omitted as we are only interested in terms up to and including $O(\epsilon)$.

To find the initial condition for the function ϕ_1^\pm , we substitute (17) into (3) and comparing terms at $O(\epsilon)$, taking account of (52). Similarly, we can substitute (18) into (4) and take account of (56) to find an initial condition for ϕ_2^\pm . Therefore

$$\phi_1^\pm = \frac{1}{2} \left(J_1^\pm \mp \int_{-L}^{\xi_\pm} K_1(\sigma) d\sigma \right) - \tilde{\phi}_1^\pm, \quad (62)$$

$$\phi_2^\pm = \frac{1}{2c} \left(J_2^\pm \mp \int_{-L}^{v_\pm} K_2(\sigma) d\sigma \right) - \tilde{\phi}_2^\pm, \quad (63)$$

where

$$\begin{aligned} J_1 &= \frac{\tilde{\omega}^2 \rho_1}{2} (f_1^- + f_1^+) + \frac{\tilde{\omega}^2 \rho_1^2}{2} (f_{1\xi_-\xi_-}^- + f_{1\xi_+\xi_+}^+) - h_{1c} - \frac{\delta}{c^2 - 1} \int_{-L}^{v_-} \int_{-L}^{v_+} f_2^-(u, T) du dv - \frac{\delta}{c^2 - 1} \int_{-L}^{v_+} \int_{-L}^{v_-} f_2^+(u, T) du dv, \\ K_1 &= f_{1T}^- + f_{1T}^+ - \frac{\tilde{\omega}^2 \rho_1}{2} (f_{1\xi_-}^- - f_{1\xi_+}^+) + \frac{\tilde{\omega}^2 \rho_1^2}{2} (f_{1\xi_-\xi_-}^- - f_{1\xi_+\xi_+}^+) - h_{1c\xi_-} + h_{1c\xi_+} \\ &- \frac{c\delta}{c^2 - 1} \int_{-L}^{v_-} f_2^-(y, T) dy + \frac{c\delta}{c^2 - 1} \int_{-L}^{v_+} f_2^+(y, T) dy, \end{aligned} \quad (64)$$

$$\begin{aligned} J_2 &= -\frac{\tilde{\omega}^2 \rho_2}{2c} (f_2^- + f_2^+) + \frac{\tilde{\omega}^2 \rho_2^2}{2} (f_{2v_-v_-}^- + f_{2v_+v_+}^+) - h_{2c} + \frac{\gamma}{c^2 - 1} \int_{-L}^{\xi_-} \int_{-L}^{\xi_+} f_1^-(y, T) dy dz + \frac{\gamma}{c^2 - 1} \int_{-L}^{\xi_+} \int_{-L}^{\xi_-} f_1^+(y, T) dy dz, \\ K_2 &= f_{2T}^- + f_{2T}^+ + \frac{\tilde{\omega}^2 \rho_2}{2} (f_{2v_-}^- - f_{2v_+}^+) + \frac{c\tilde{\omega}^2 \rho_2^2}{2} (f_{2v_-v_-}^- - f_{2v_+v_+}^+) - ch_{2cv_-} + ch_{2cv_+} \\ &+ \frac{\gamma}{c^2 - 1} \int_{-L}^{\xi_-} f_1^-(y, T) dy - \frac{\gamma}{c^2 - 1} \int_{-L}^{\xi_+} f_1^+(y, T) dy, \end{aligned} \quad (65)$$

$$\tilde{\phi}_1^\pm = \int_{-L}^L \frac{1}{2} \left(J_1^\pm \mp \int_{-L}^{\xi_\pm} K_1(\sigma) d\sigma \right) d\xi_\pm, \quad \tilde{\phi}_2^\pm = \int_{-L}^L \frac{1}{2c} \left(J_2^\pm \mp \int_{-L}^{v_\pm} K_2(\sigma) d\sigma \right) dv_\pm. \quad (66)$$

We now have expressions up to $O(\varepsilon)$, however we still need to find an equation governing $\phi_{1,2}^\pm$, therefore we compare terms at $O(\varepsilon^2)$, taking account of all previous results. All coupling terms between left- and right-propagating waves are gathered

in one function, and terms of the type of (41) and (44) are gathered in another function for convenience, as we do not require them to determine $\phi_{1,2}^\pm$. Gathering terms at $O(\varepsilon^2)$ we have

$$\begin{aligned}
 -4S_{1\xi_-\xi_+} &= -f_{1TT}^- - f_{1TT}^+ - 2g_{1\tau T}^- - 2g_{1\tau T}^+ - h_{1\tau\tau}^- - h_{1\tau\tau}^+ + 2h_{1\xi_-\tau}^- - 2h_{1\xi_+\tau}^+ + 2\psi_{1\xi_-\tau}^- - 2\psi_{1\xi_+\tau}^+ + (f_1^- h_1^-)_{\xi_-\xi_+} + (f_1^+ h_1^+)_{\xi_+\xi_+} \\
 &\quad + \frac{1}{2} (g_1^-)_{\xi_-\xi_+} + \frac{1}{2} (g_1^+)_{\xi_+\xi_+} + h_{1\xi_-\xi_-\xi_+} + h_{1\xi_+\xi_+\xi_+} + (d_1 + d_2 \delta \cos(\tilde{\omega}\tau)) (h_{1\xi_-\xi_+}^- + h_{1\xi_+\xi_+}^+) \\
 &\quad - 2g_{1\xi_-\xi_-\tau}^- + 2g_{1\xi_+\xi_+\tau}^+ - 2f_{1\xi_-\xi_-\tau}^- + 2f_{1\xi_+\xi_+\tau}^+ - \delta (h_1^- - h_2^- + h_1^+ - h_2^+) - 4\mu_{1c} - 4\Upsilon_1, \quad (67) \\
 -4c^2 S_{2v_-\nu_+} &= -f_{2TT}^- - f_{2TT}^+ - 2g_{2\tau T}^- - 2g_{2\tau T}^+ - h_{2\tau\tau}^- - h_{2\tau\tau}^+ + 2ch_{2v_-\tau}^- - 2ch_{2v_+\tau}^+ + 2c\psi_{2v_-\tau}^- - 2c\psi_{2v_+\tau}^+ \\
 &\quad + \alpha (f_2^- h_2^-)_{v_-\nu_+} + \alpha (f_2^+ h_2^+)_{v_+\nu_+} + \frac{\alpha}{2} (g_2^-)_{v_-\nu_+} + \frac{\alpha}{2} (g_2^+)_{v_+\nu_+} + \alpha (d_1 - d_2 \gamma \cos(\tilde{\omega}\tau)) (h_{2v_-\nu_+}^- + h_{2v_+\nu_+}^+) \\
 &\quad + \beta c^2 h_{2v_-\nu_-\nu_+}^- + \beta c^2 h_{2v_+\nu_+\nu_+}^+ - 2\beta c g_{2v_-\nu_-\tau}^- + 2\beta c g_{2v_+\nu_+\tau}^+ - 2\beta c f_{2v_-\nu_-\tau}^- + 2\beta c f_{2v_+\nu_+\tau}^+ \\
 &\quad + \gamma (h_1^- - h_2^- + h_1^+ - h_2^+) - 4\mu_{2c} - 4\Upsilon_2, \quad (68)
 \end{aligned}$$

where μ_{1c} and μ_{2c} are the coupling terms at this order, while Υ_1 and Υ_2 are the terms involving \hat{f}_2 or equivalent. We average (67) at constant ξ_- or constant ξ_+ , or average (68) at constant v_- or constant v_+ , integrate with respect to τ and rearrange to obtain

$$\begin{aligned}
 2\psi_{1\xi_\pm} &= H_1^\pm(\xi_\pm, \tau, T) + \hat{H}_1^\pm(\xi_\pm, T) \tau, \\
 2c\psi_{2v_\pm} &= H_2^\pm(v_\pm, \tau, T) + \hat{H}_2^\pm(v_\pm, T) \tau, \quad (69)
 \end{aligned}$$

where the functions $H_{1,2}^\pm, \hat{H}_{1,2}^\pm$ can be found from (67) or (68). To avoid secular terms we require that $\hat{H}_{1,2}^\pm = 0$ and this allows us to find equations for $\phi_{1,2}^\pm$. Therefore we look for terms in (67) that depend only on ξ_\pm and T . Following this approach we obtain

$$\begin{aligned}
 (\mp 2\phi_{1T}^\pm + (f_1^\pm \phi_1^\pm)_{\xi_\pm} + d_1 \phi_{1\xi_\pm}^\pm + \phi_{1\xi_\pm \xi_\pm}^\pm)_{\xi_\pm} &= \delta \phi_1^\pm \\
 + f_{1TT}^\pm \mp 2f_{1\xi_\pm \xi_\pm}^\pm + \frac{\tilde{\omega}^2 \tilde{\theta}_1^2}{2} f_{1\xi_\pm \xi_\pm}^\pm - \frac{\tilde{\theta}_1^2}{2} (f_{1\xi_\pm}^{\pm 2})_{\xi_\pm \xi_\pm}, \quad (70)
 \end{aligned}$$

and from (68) we have

$$\begin{aligned}
 (\mp 2c\phi_{2T}^\pm + \alpha (f_2^\pm \phi_2^\pm)_{v_\pm} + \alpha d_1 \phi_{2v_\pm}^\pm + \beta c^2 \phi_{2v_\pm v_\pm}^\pm)_{v_\pm} &= \gamma \phi_2^\pm \\
 + f_{2TT}^\pm \mp 2c\beta f_{2v_\pm v_\pm}^\pm + \frac{\tilde{\omega}^2 \tilde{\theta}_2^2}{2} f_{2v_\pm v_\pm}^\pm - \frac{\alpha \tilde{\theta}_2^2}{2} (f_{2v_\pm}^{\pm 2})_{v_\pm v_\pm}, \quad (71)
 \end{aligned}$$

where

$$\tilde{\theta}_1 = \frac{\theta_1}{\sin(\tilde{\omega}\tau)} = \frac{d_2 \delta}{2\tilde{\omega}}, \quad \tilde{\theta}_2 = \frac{\theta_2}{\sin(\tilde{\omega}\tau)} = \frac{\alpha d_2 \gamma}{2c\tilde{\omega}}. \quad (72)$$

We have now defined all functions up to and including $O(\varepsilon)$ and so stop our derivation, however in theory this could be continued to any order. We also note that every function in this expansion has been constructed to have zero mean, either directly or by the appropriate choice of integration constant.

III. VALIDITY OF WEAKLY-NONLINEAR SOLUTION

In Section II we constructed the weakly-nonlinear solution to the original cRB equations (1) - (4), when the characteristic speeds are essentially distinct (high-contrast case). We now confirm the validity of the constructed expansions by numerically solving the system (1) - (2) and comparing this direct numerical solution to the constructed solution (17) and (18) with an increasing number of terms included. This was constructed in Section II, so we need to solve (22), (23) for the leading-order solution and (70), (71) for the solution up to and including terms at $O(\varepsilon)$.

In order to numerically solve these equations, in this section and the subsequent sections, we implement three pseudo-spectral numerical schemes described in Supplementary Materials. For the coupled Boussinesq equations we use the methods in Appendix A and for a single Ostrovsky equation and we use the method in Appendix B, both of which are similar to schemes in Ref. 13. We use a modified pseudo-spectral scheme for the coupled Ostrovsky equations, based upon²¹, to allow for larger time steps to be taken, and this is presented in Appendix C. We note that the choice of integration constants to maintain zero mean is conveniently implemented within the pseudo-spectral scheme by setting the coefficient of the zero harmonic to zero.

Unless stated otherwise, we assume that $\Delta x = 0.1$, $\Delta t = 0.01$ and $\Delta T = \varepsilon \Delta t$. In some calculations these parameters may be changed to obtain a higher accuracy result and this will be stated in the figure captions. The domain is taken as $[-L, L]$ in all cases, with $L = 300$ for most calculations with solitary waves and $3 \times L_K$ for cnoidal waves, where L_K is the period of the cnoidal wave.

In all subsequent calculations, we shall refer to the solution of the system (1) - (2) as the numerical solution of the exact system and compare this to the weakly-nonlinear solution

with an increasing number of terms included. We calculate the solution in the domain $x \in [-40, 40]$ and for $t \in [0, \hat{T}]$ where $\hat{T} = 1/\varepsilon$.

To construct a right-propagating wave as the initial condition, with no left-propagating wave, we choose our functions F and V appropriately so that $f_1^- = F_1$, $f_2^- = F_2$ and $f_1^+ = f_2^+ = 0$. Explicitly, for solitary wave initial conditions, we have

$$\begin{aligned} F_1(x) &= A_1 \operatorname{sech}^2\left(\frac{x}{\Lambda_1}\right) + p, & F_2(x) &= A_2 \operatorname{sech}^2\left(\frac{x}{\Lambda_2}\right), \\ V_1(x) &= 2\frac{A_1}{\Lambda_1} \operatorname{sech}^2\left(\frac{x}{\Lambda_1}\right) \tanh\left(\frac{x}{\Lambda_1}\right), \\ V_2(x) &= 2c\frac{A_2}{\Lambda_2} \operatorname{sech}^2\left(\frac{x}{\Lambda_2}\right) \tanh\left(\frac{x}{\Lambda_2}\right), \end{aligned} \quad (73)$$

where p is a constant and we have

$$\begin{aligned} A_1 &= 6k_1^2, & \Lambda_1 &= \sqrt{2}/k_1, & k_1 &= 1/\sqrt{6}, \\ A_2 &= 6ck_2^2/\alpha, & \Lambda_2 &= \sqrt{2c\beta}/k_2, & k_2 &= \sqrt{\alpha/6c}. \end{aligned}$$

We have added a pedestal to the initial condition for u to have distinct non-zero values for d_1 and d_2 .

To determine the agreement between the numerical solution of the exact system and the weakly-nonlinear solution, we calculate the error as

$$e^{(i)} = \log \left| 1 - \frac{v_i}{v} \right|, \quad i = 1, 2, 3, \quad (74)$$

where v is the numerical solution of the exact system, the weakly-nonlinear solution (17), (18) with only leading order terms included as v_1 , with terms up to and including $O(\sqrt{\varepsilon})$ as v_2 and with terms up to and including $O(\varepsilon)$ as v_3 . This will be plotted alongside v for comparison.

We choose $\alpha = \beta = c = 2$, $\delta = \gamma = 0.5$, $p = 7$ and present the comparison between the numerical solution of the exact system and weakly-nonlinear solutions, at various orders of ε , for u in Figure 1. A similar result can be observed for w . We see from the error lines that the leading order solution (red, dashed line) is reasonably accurate, with an error of less than 0.02. This is improved with the addition of the $O(\sqrt{\varepsilon})$ terms (black, dash-dotted line), reducing the phase shift around the main wave packet. The inclusion of $O(\varepsilon)$ terms (green, dotted line) reduces the error by an order of magnitude, as expected. We only present one example here for brevity, but the same results have been observed for multiple values of δ , γ , pedestal height p , and for w .

To further confirm the validity of the solution, we calculate the maximum absolute error over x as

$$r_i = \max_{-L \leq x \leq L} |v(x, t) - v_i(x, t)|, \quad i = 1, 2, 3. \quad (75)$$

This error is calculated at every time step and, to smooth the oscillations in the errors we average r_i in the final third of the calculation, denoting this value as \hat{r}_i . We then use a least-squares power fit to determine how the maximum absolute error varies with the small parameter ε . Therefore we write the errors in the form

$$\exp[\hat{r}_i] = C_i \varepsilon^{\alpha_i}, \quad (76)$$

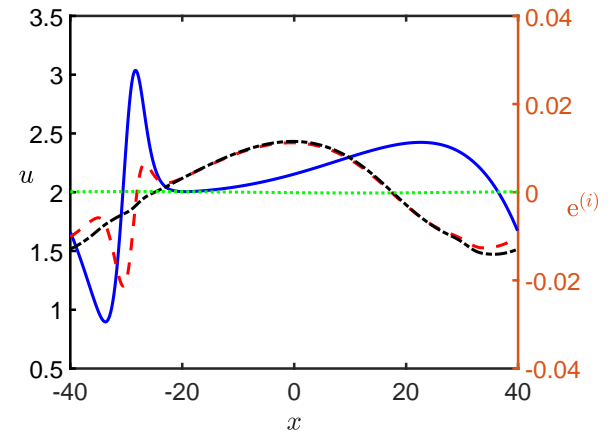


FIG. 1. A result of the direct numerical simulation (solid, blue) and comparison of the errors between this solution and the weakly-nonlinear solution, including leading order (dashed, red), $O(\sqrt{\varepsilon})$ (dash-dot, black) and $O(\varepsilon)$ (dot, green) corrections, at $t = 1/\varepsilon$, for u . Parameters are $L = 40$, $N = 800$, $k = 1/\sqrt{6}$, $\alpha = \beta = c = 2$, $\gamma = 0.5$, $p = 7$, $\varepsilon = 2.38 \times 10^{-3}$, $\Delta t = 0.01$ and $\Delta T = \varepsilon \Delta t$. The solution agrees well to leading order and this agreement is improved with the addition of higher-order corrections.

and take the logarithm of both sides to form the error plot.

The corresponding errors for the cases considered in Figure 1 are plotted in Figure 2. The slope of the curves is approxi-

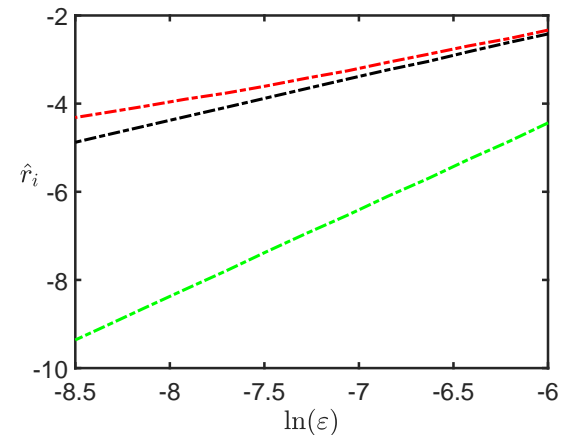


FIG. 2. A comparison of error curves for varying values of ε , at $t = 1/\varepsilon$, for the weakly-nonlinear solution including leading order (upper, red), $O(\sqrt{\varepsilon})$ (middle, black) and $O(\varepsilon)$ (lower, green) corrections for u . Parameters are $L = 40$, $N = 800$, $k = 1/\sqrt{6}$, $\alpha = \beta = c = 2$, $\gamma = 0.5$, $\Delta t = 0.01$ and $\Delta T = \varepsilon \Delta t$. The inclusion of more terms in the expansion increases the accuracy.

mately 0.77, 0.99 and 1.96, which are slightly higher than the theoretical values for the inclusion of leading order terms and the case with terms up to and including $O(\varepsilon)$ terms. However this can be explained by the solutions in this case being

wave packets, so a phase shift at the level of $O(\sqrt{\varepsilon})$ will not have as much of an effect on the errors as it would for radiating solitary waves.²⁰ Furthermore, the increase in the slope is consistent with the results seen for previous studies for the Boussinesq-Klein-Gordon equation.¹³

IV. COUNTER-PROPAGATING WAVES

We now consider various cases for wave interaction, where we will use the constructed weakly-nonlinear solution with the inclusion of terms up to $O(\sqrt{\varepsilon})$ to take account of the mass. Two types of initial condition are considered: solitary wave and cnoidal wave. While our focus is on the high-contrast case (when $c - 1 = O(1)$), it is instructive to compare with the solutions emerging in the low-contrast case (when $c - 1 = O(\varepsilon)$). The results for the low-contrast case are presented using the solution obtained in Ref. 20. Then, we discuss the solutions for the high-contrast case, whose weakly-nonlinear solution was constructed in Section II.

A. Solitary Wave Initial Condition

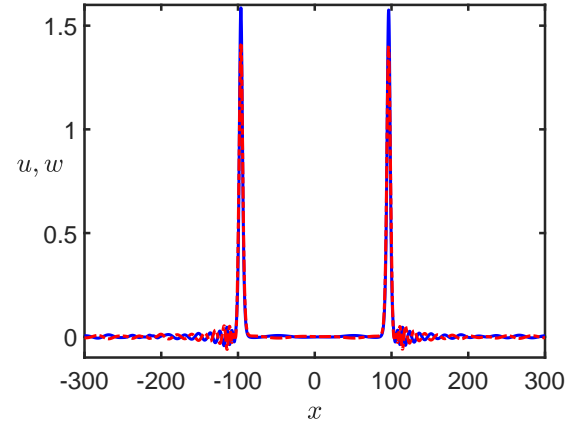
Firstly we take solitary wave initial conditions, as was done in Section III. For counter-propagating waves, we introduce a second wave, with the same parameters as the first wave, at a phase shift with a sign change in V to result in wave propagation to the left for the second wave. Explicitly we have

$$\begin{aligned} F_i(x) &= A_i \operatorname{sech}^2\left(\frac{x+x_0}{\Lambda_i}\right) + A_i \operatorname{sech}^2\left(\frac{x+x_1}{\Lambda_i}\right), \\ V_i(x) &= 2\frac{A_i}{\Lambda_i} \operatorname{sech}^2\left(\frac{x+x_0}{\Lambda_i}\right) \tanh\left(\frac{x+x_0}{\Lambda_i}\right) \\ &\quad - 2\frac{A_i}{\Lambda_i} \operatorname{sech}^2\left(\frac{x+x_1}{\Lambda_i}\right) \tanh\left(\frac{x+x_1}{\Lambda_i}\right), \end{aligned} \quad (77)$$

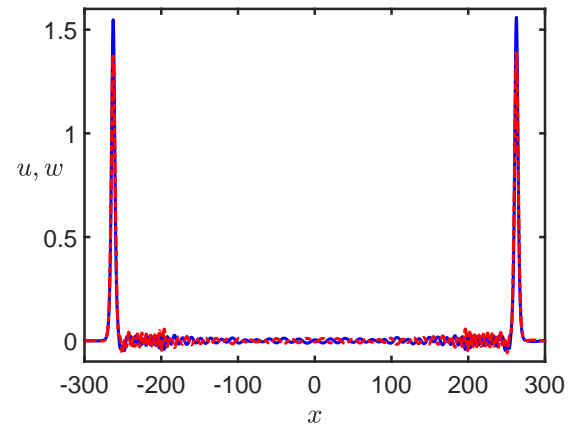
where $i = 1$ is the initial condition for u and $i = 2$ is the initial condition for w and A_i, Λ_i are as defined in (73). These can then be used to give initial conditions for the constructed weakly-nonlinear solution via (26) and (27).

1. Low-contrast case

We analyse the case when the characteristic speeds in the equations are close, so we have $c - 1 = O(\varepsilon)$ and the periodic domain is sufficiently large. The solutions in this case are expected to be radiating solitary waves.²⁰ We take the initial condition (77), where the waves will be well separated via the choice of x_0 and x_1 . To determine the behaviour of the solution, we consider it at two times: $t = 150$, before interaction, and $t = 500$, after the interaction. The results are shown in Figure 3. Firstly we see that the solitons form a solitary wave with a co-propagating radiating tail, as expected from the co-propagating case.²⁰ As they interact the solitons appear to emerge with only a small change in their amplitudes,



(a) Weakly-nonlinear solution to cRB equations at $t = 150$.

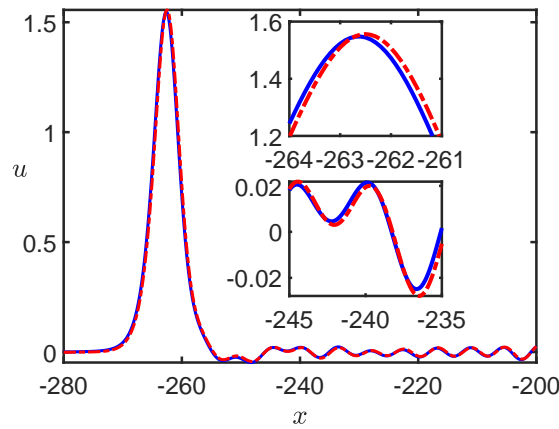


(b) Weakly-nonlinear solution to cRB equations at $t = 500$.

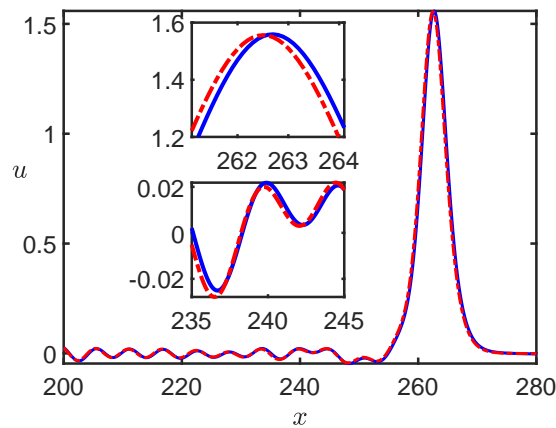
FIG. 3. Solution for counter-propagating waves in the cRB equations, using the weakly-nonlinear solution including terms up to $O(\sqrt{\varepsilon})$, at (a) $t = 150$ and (b) $t = 500$. Parameters are $L = 300$, $N = 6000$, $\varepsilon = 0.05$, $\alpha = \beta = 1.05$, $c = 1.025$, $\delta = \gamma = 1$, $k_1 = 1/\sqrt{2}$, $k_2 = \sqrt{1.05/2}$, $x_0 = 250$, $x_1 = -250$, $\Delta t = 0.01$ and $\Delta T = \varepsilon \Delta t$. Here, u/w are shown by blue, solid/red, dashed curves, respectively.

although the amplitude can decay in the evolution of the radiating solitary wave. To determine if their collision is elastic or does indeed introduce a small change in amplitude, or perhaps a phase shift, we compare the solution in the counter-propagating case to a corresponding one when there is only one radiating solitary wave present.

The comparison between the cases with and without interaction are shown in Figure 4 for u , while a similar result is seen for w and so is omitted for brevity. We can clearly see that a small phase shift occurs once interaction has taken place (blue, solid line) and the amplitude is also slightly reduced on the peak, suggesting that this interaction is not elastic, in contrast to the case with solitary waves. However, the difference is small, and the interaction is only weakly-inelastic.



(a) Left-propagating radiating solitary wave for u at $t = 500$.



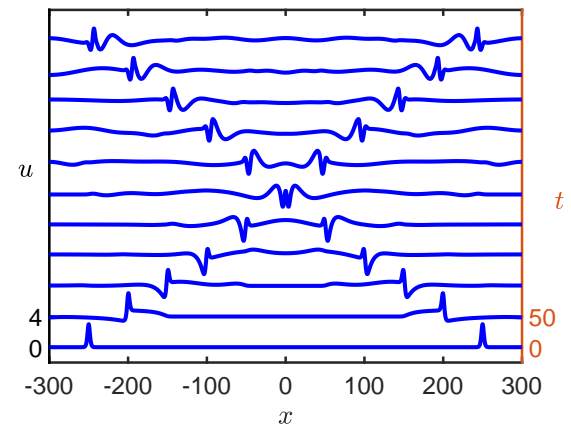
(b) Right-propagating radiating solitary wave for u at $t = 500$.

FIG. 4. A small phase shift appears as a result of the interaction of radiating solitary waves (blue, solid line) and the case without interaction (red, dashed line), for u at $t = 500$, enhanced for the (a) left-propagating wave, and (b) right-propagating wave. Parameters are $L = 300$, $N = 6000$, $\varepsilon = 0.05$, $\alpha = \beta = 1.05$, $c = 1.025$, $\delta = \gamma = 1$, $k_1 = 1/\sqrt{2}$, $k_2 = \sqrt{1.05/2}$, $x_0 = 250$, $x_1 = -250$, $\Delta t = 0.01$ and $\Delta T = \varepsilon \Delta t$.

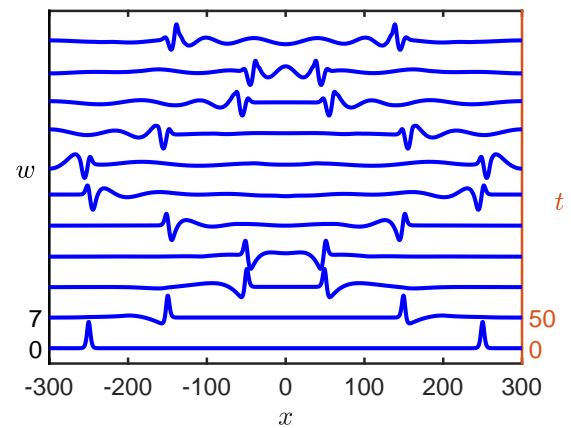
2. High-contrast case

Now we consider the case when the characteristic speeds in the equations are distinct, so we have $c - 1 = O(1)$, and we consider the effect of wave interaction on wave packets. The initial condition is taken as (77) and we analyse the interaction of the generated wave packets. The results are presented in Figure 5. Wave packets are generated in both layers with the packet generated in the lower layer moving faster than the corresponding packet in the upper layer. At the point of interaction the packets move through each other and emerge with the appearance of small changes in their shape and structure, which could be attributed to evolution of the wave packets.

As was done in the low-contrast case, we compare the result of the interaction to the corresponding co-propagating case



(a) Solution for u at multiple times.



(b) Solution for w at multiple times. The wave moves twice as fast in this case.

FIG. 5. Comparison of counter-propagating wave packets at multiple times, for (a) u and (b) w . Parameters are $L = 300$, $N = 6000$, $\varepsilon = 0.0005$, $\alpha = \beta = c = 2$, $\delta = \gamma = 1$, $k_1 = 1/\sqrt{2}$, $k_2 = 1$, $x_0 = 250$, $x_1 = -250$, $\Delta t = 0.01$ and $\Delta T = \varepsilon \Delta t$.

without interaction. The comparison is shown in Figure 6 for u , and again we see a similar result for w , albeit at a different position due to the different characteristic speeds, so we omit it here. We see that interaction (blue, solid line) leads to several changes, in particular the wave packet is linked to the other wave packet in the case of interaction, leading to a number of differences between the solutions. Therefore, the collision is strongly inelastic in the high-contrast case.

B. Cnoidal Wave Initial Condition

A second case of interest is using a cnoidal wave as the initial condition for the cRB equations. We can obtain the cnoidal wave initial condition by considering the uncoupled

This is the author's peer reviewed, accepted manuscript. However, the online version of record will be different from this version once it has been copyedited and typeset. PLEASE CITE THIS ARTICLE AS DOI: 10.1063/5.0112982

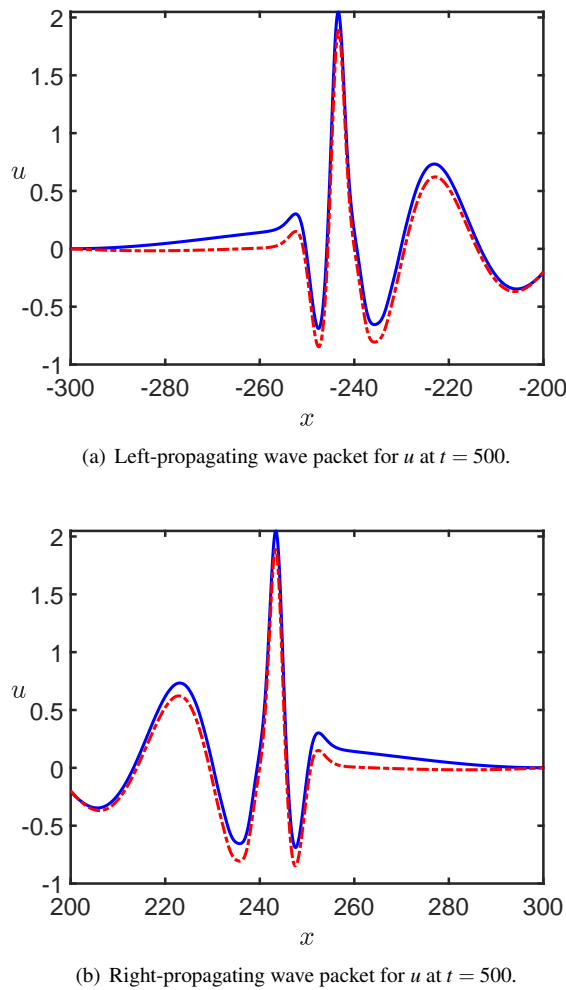


FIG. 6. Significant differences appear as a result of the interaction of wave packets (blue, solid line) and the case without interaction (red, dashed line), for u at $t = 500$, enhanced for the (a) left-propagating wave, and (b) right-propagating wave. Parameters are $L = 300$, $N = 6000$, $\varepsilon = 0.0005$, $\alpha = \beta = c = 2$, $\delta = \gamma = 1$, $k_1 = 1/\sqrt{2}$, $k_2 = 1$, $x_0 = 250$, $x_1 = -250$, $\Delta t = 0.01$ and $\Delta T = \varepsilon \Delta t$.

equations for u and w , for example

$$w_{tt} - c^2 w_{xx} = \varepsilon \left[\frac{\alpha}{2} (w^2)_{xx} + \beta w_{ttxx} \right] \quad (78)$$

for w , and the equation for u can be found by setting $c = \alpha = \beta = 1$. The leading-order weakly-nonlinear solution to this equation takes the form of the KdV equation

$$2cf_T + \alpha f f_\xi + \beta c^2 f_\xi \xi_\xi = 0, \quad (79)$$

where we have assumed that $\xi = x - ct$ and $T = \varepsilon t$. This can be thought of as a truncated Ostrovsky equation derived in Section II, under the assumption that the initial condition has zero mean. The cnoidal wave solution to this equation can be

obtained as

$$f = -\frac{6\beta c^2}{\alpha} \left(f_2 - (f_2 - f_3) \text{cn}^2 \left[(\xi + vT) \sqrt{\frac{f_1 - f_3}{2}} |m| \right] \right), \quad (80)$$

where

$$v = (f_1 + f_2 + f_3)\beta c, \quad m = \frac{f_2 - f_3}{f_1 - f_3}.$$

The solution is parametrised by the three constants $f_3 < f_2 < f_1$ with $0 < m < 1$. The wave length of the cnoidal wave is given by

$$L_K = 2K(m) \sqrt{\frac{2}{f_1 - f_3}}, \quad (81)$$

where

$$K(m) = \int_0^{\pi/2} \frac{d\theta}{\sqrt{1 - m \sin^2 \theta}}$$

is the complete elliptic integral of the first kind. This wave is an exact solution to the KdV equation and a natural initial condition for the cRB equations, in the same way as the solitary wave solution in Section IV A also was a natural initial condition since the Ostrovsky equation is an extension of the KdV equation.

To reduce the number of parameters in the solution, we will assume that $f_2 = 0$, which means that the cnoidal wave is moving on a zero background. This will reduce the magnitude of the mean term, but it will not be zero, which is consistent with the approach for the solitary wave solution. To simplify notation we introduce the constant $\theta = \sqrt{\frac{f_1 - f_3}{2}}$ and variable $\tilde{x} = x + x_0$.

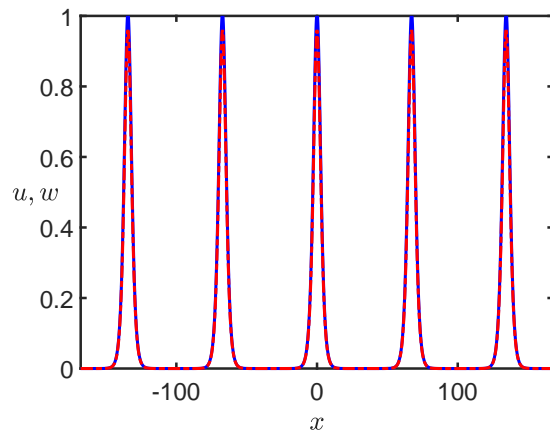
To construct a right-propagating cnoidal wave as the initial condition, we choose our functions F and V appropriately, as was done for the solitary wave initial conditions. Explicitly for the co-propagating wave we have the initial condition

$$\begin{aligned} F_1(x) &= -6f_3 \text{cn}^2[\theta \tilde{x}|m], & F_2(x) &= -\frac{6\beta c^2}{\alpha} f_3 \text{cn}^2[\theta \tilde{x}|m], \\ V_1(x) &= -12f_3 \theta \text{cn}[\theta \tilde{x}|m] \text{sn}[\theta \tilde{x}|m] \text{dn}[\theta \tilde{x}|m], \\ V_2(x) &= -\frac{12\beta c^2}{\alpha} f_3 \theta \text{cn}[\theta \tilde{x}|m] \text{sn}[\theta \tilde{x}|m] \text{dn}[\theta \tilde{x}|m]. \end{aligned} \quad (82)$$

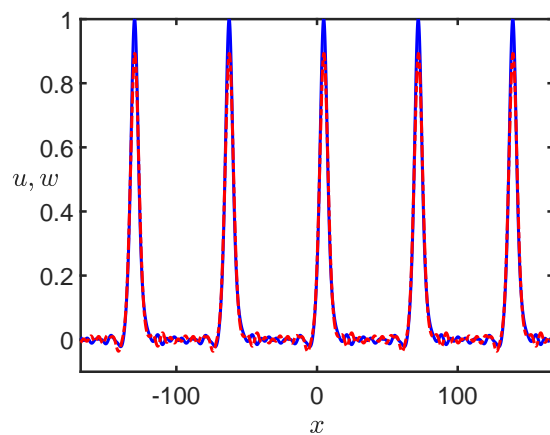
1. Low-contrast case

Firstly we consider the low-contrast case. Our earlier results would suggest that each peak in the cnoidal wave will evolve into a radiating solitary wave, whose tail will eventually interact with the preceding wave. We take the initial condition for co-propagating waves, given in (82), and the results are presented in Figure 7.

As the troughs of the cnoidal wave are long, we can see the generation of a co-propagating radiating tail forming behind the cnoidal wave peaks, which then begins to interact with the



(a) Solution at $t = 0$.

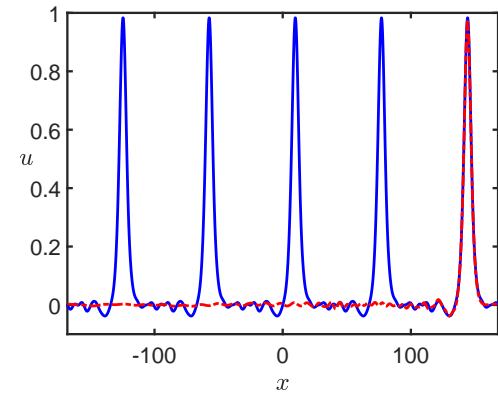


(b) Solution at $t = 400$.

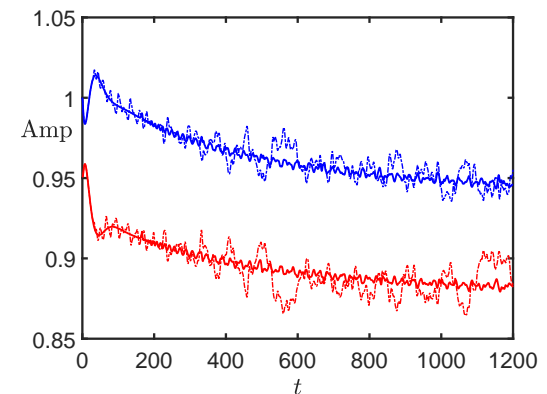
FIG. 7. Generation of co-propagating radiating solitary waves from a cnoidal wave initial condition, for u (blue, solid line) and w (red, dashed line), at (a) $t = 0$, and (b) $t = 400$. Parameters are $L \approx 168.0$, $N = 3360$, $\varepsilon = 0.05$, $f_1 = 1 \times 10^{-8}$, $f_2 = 0$, $f_3 = -\frac{1}{6}$, $\alpha = \beta = 1$, $c = 1.025$, $\delta = \gamma = 1$, $x_0 = 0$, $\Delta t = 0.01$ and $\Delta T = \varepsilon \Delta t$.

preceding peak. The peaks of the wave appear to survive this interaction and maintain their shape, with a small reduction in amplitude that could be attributed to the generation of the radiating tail. The waves appear to form a larger wave structure across the domain.

We can consider the effect of interaction of the peaks with the radiating tails by running a simulation for the same initial condition, with five peaks, shown in Figure 7, and compare this with a truncated initial condition consisting of only a single peak, but with the same domain size as our previous simulation. This is shown in Figure 8. From Figure 8(a) we can see that there is not a significant phase shift in the leading peak, however we see several phase shifts and amplitude changes have occurred with the tail, caused by the interaction between the tails and the peaks. In Figure 8(b) we can see that the amplitude of the peak in the case without interaction follows a fairly steady path, while in the case with interaction



(a) Solution at $t = 800$ for u .



(b) Amplitude of case with (dashed line) and without (solid line) interaction.

FIG. 8. Comparison of effect of peak interaction with radiating tails. In (a) we have a cnoidal wave with multiple peaks (blue, solid line) and a cnoidal wave with a single peak (red, dashed line). In (b) the peak amplitude in the single peak case (solid line) and multiple peak case (dashed line), for u (blue) and w (red). Parameters are $L \approx 168.0$, $N = 3360$, $\varepsilon = 0.05$, $f_1 = 1 \times 10^{-8}$, $f_2 = 0$, $f_3 = -\frac{1}{6}$, $\alpha = \beta = 1$, $c = 1.025$, $\delta = \gamma = 1$, $x_0 = 0$, $\Delta t = 0.01$ and $\Delta T = \varepsilon \Delta t$.

it has large changes caused by interactions with the radiated tail of the preceding peak. This is qualitatively similar to the effects of a large soliton tunnelling through a soliton gas or other oscillatory wave structure (see, for example, Refs. 22, 23 and references therein), but in this case there are no significant phase-shifts, and the main effect is seen in the amplitude variations.

2. High-contrast case

Following on from Section IV A, we now examine the case when the characteristic speeds in the equations are distinct, so we have $c - 1 = O(1)$. We take the initial condition (82) and the results are presented in Figure 9. A wave packet is formed by each peak of the cnoidal wave, which were chosen to be approximately 100 units apart so that the peaks of the

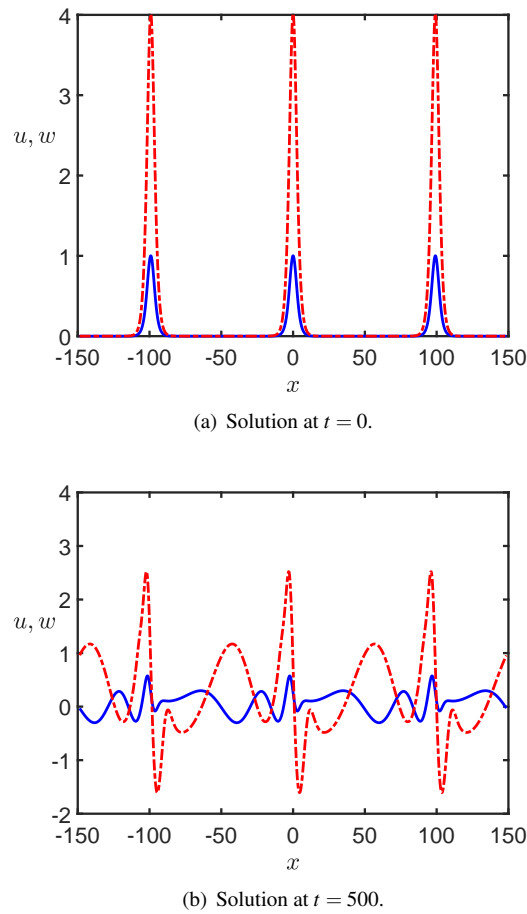


FIG. 9. Generation of wave packets from a cnoidal wave initial condition, for u (blue, solid line) and w (red, dashed line), at (a) $t = 0$, and (b) $t = 500$. Parameters are $L \approx 148.6$, $N = 2974$, $\varepsilon = 0.005$, $f_1 = 1 \times 10^{-12}$, $f_2 = 0$, $f_3 = -\frac{1}{6}$, $\alpha = \beta = 2$, $c = 2$, $\delta = \gamma = 1$, $x_0 = 0$, $\Delta t = 0.01$ and $\Delta T = \varepsilon \Delta t$.

cnoidal wave are distinct and each wave packet can be seen clearly. Note that, although the solutions for u and w overlay each other, the packets formed in the lower layer move faster than the upper layer and their overlap is due to the choice of time. The wave packets are connecting to each other in the intervening space between the main wave packets.

To further explore the evolution of the cnoidal wave initial condition into a series of wave packets, we choose an initial condition when the peaks of the cnoidal wave are approximately 50 units apart. This is plotted in Figure 10. We can

see that wave packets are again generated, however in this case the qualitative structure is different and the connection between the wave packets is shorter.

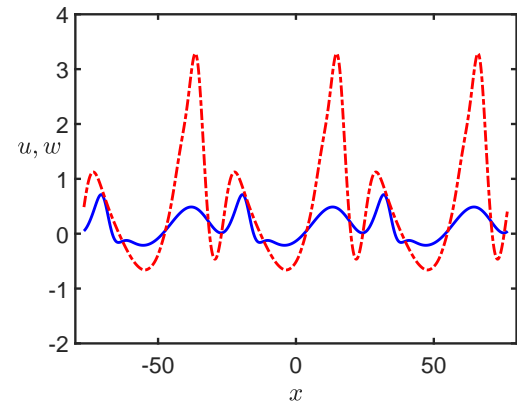


FIG. 10. Generation of wave packets from a cnoidal wave initial condition, for u (blue, solid line) and w (red, dashed line), at $t = 500$. Parameters are $L \approx 76.9$, $N = 1538$, $\varepsilon = 0.005$, $f_1 = 1 \times 10^{-6}$, $f_2 = 0$, $f_3 = -\frac{1}{6}$, $\alpha = \beta = 2$, $c = 2$, $\delta = \gamma = 1$, $x_0 = 0$, $\Delta t = 0.01$ and $\Delta T = \varepsilon \Delta t$.

V. CONSERVATION LAWS

The system (1) - (2) is related to the system

$$U_{tt} - U_{xx} = \varepsilon [U_x U_{xx} + U_{ttxx} - \delta (U - W)], \quad (83)$$

$$W_{tt} - c^2 W_{xx} = \varepsilon [\alpha W_x W_{xx} + \beta W_{ttxx} + \gamma (U - W)], \quad (84)$$

$$U(x, t) = \int_{-L}^x u(\sigma, t) d\sigma, \quad W(x, t) = \int_{-L}^x w(\sigma, t) d\sigma.$$

It naturally follows that $U(-L) = W(-L) = 0$, and also that $U_t(-L) = W_t(-L) = 0$, which will be used in what follows. The system (83) - (84) is Lagrangian, and it has three local conservation laws for the mass, energy and momentum.¹⁰ Using these known conservation laws, we can find the conservation laws for our system (1) - (2) in the form of one local (mass) and two non-local (energy and momentum) conservation laws. Indeed, differentiating the conservation law for mass from Ref. 10 with respect to x and rewriting the energy and momentum laws in terms of u , w instead of U_x , W_x we obtain

$$\left(u_t + \frac{\delta}{\gamma} w_t\right)_t - \left(u_x + \frac{\delta c^2}{\gamma} w_x + \varepsilon u u_x + \frac{\varepsilon \alpha \delta}{\gamma} w w_x + u_{tt} + \frac{\varepsilon \beta \delta}{\gamma} w_{tt}\right)_x = 0, \quad (85)$$

$$\frac{1}{2} \left\{ U_t^2 + \frac{\delta}{\gamma} W_t^2 + u^2 + \frac{\delta c^2}{\gamma} w^2 + \frac{\varepsilon}{3} \left(u^3 + \frac{\alpha \delta}{\gamma} w^3 \right) + \varepsilon u_t^2 + \frac{\varepsilon \beta \delta}{\gamma} w_t^2 + \varepsilon \delta (U - W)^2 \right\}_t$$

$$- \left(U_t u + \frac{\delta c^2}{\gamma} W_t w + \frac{\varepsilon}{2} U_t u^2 + \frac{\varepsilon \alpha \delta}{2\gamma} W_t w^2 + \varepsilon U_t u_{tt} + \frac{\varepsilon \beta \delta}{\gamma} W_t w_{tt} \right)_x = 0, \quad (86)$$

$$\left(U_t u + \frac{\delta}{\gamma} W_t w + \varepsilon u_t u_x + \frac{\varepsilon \beta \delta}{\gamma} w_t w_x \right)_t - \left\{ \varepsilon u u_{tt} + \frac{\varepsilon \beta \delta}{\gamma} w w_{tt} \right.$$

$$\left. + \frac{1}{2} \left[U_t^2 + \frac{\delta}{\gamma} W_t^2 + u^2 + \frac{\delta c^2}{\gamma} w^2 + \frac{2\varepsilon}{3} \left(u^3 + \frac{\alpha \delta}{\gamma} w^3 \right) + \varepsilon u_t^2 + \frac{\varepsilon \beta \delta}{\gamma} w_t^2 - \varepsilon \delta (U - W)^2 \right] \right\}_x = 0. \quad (87)$$

Integrating these conservation laws with respect to x from $-L$ to L , using the periodicity of u and w on $[-L, L]$, we obtain

one conserved quantity (mass)

$$\frac{d}{dt} \left(\langle u \rangle + \frac{\delta}{\gamma} \langle w \rangle \right) = 0, \quad (88)$$

and two non-local conservation laws (energy and momentum, respectively)

$$\frac{dE}{dt} = \frac{1}{2} \frac{d}{dt} \int_{-L}^L \left\{ U_t^2 + \frac{\delta}{\gamma} W_t^2 + u^2 + \frac{\delta c^2}{\gamma} w^2 + \frac{\varepsilon}{3} \left(u^3 + \frac{\alpha \delta}{\gamma} w^3 \right) + \varepsilon u_t^2 + \frac{\varepsilon \beta \delta}{\gamma} w_t^2 + \varepsilon \delta (U - W)^2 \right\} dx$$

$$= \left\{ U_t(L) \left[u(L) + \frac{\varepsilon}{2} u^2(L) + \varepsilon u_{tt}(L) \right] + W_t(L) \left[\frac{\delta c^2}{\gamma} w(L) + \frac{\varepsilon \alpha \delta}{2\gamma} w^2(L) + \frac{\varepsilon \beta \delta}{\gamma} w_{tt}(L) \right] \right\}, \quad (89)$$

$$\frac{dM}{dt} = \frac{d}{dt} \int_{-L}^L \left(U_t u + \frac{\delta}{\gamma} W_t w + \varepsilon u_t u_x + \frac{\varepsilon \beta \delta}{\gamma} w_t w_x \right) dx = \frac{1}{2} \left[U_t^2(L) + \frac{\delta}{\gamma} W_t^2(L) - \varepsilon \delta (U(L) - W(L))^2 \right]. \quad (90)$$

Note that if $\langle u \rangle = \langle w \rangle = 0$ (i.e. $d_1 = d_2 = 0$), then the non-local conservation laws (89) and (90) yield the usual (local) conservation of energy and momentum. More generally, the non-local conservation laws are applicable when the waves propagate on the background of some initially pre-strained basic state characterised by non-zero mass of u and w .

We now verify the relations (89) and (90). The parameters for the simulation are chosen as $\varepsilon = 0.01$, $c = 1.025$ and $\alpha = \beta = \delta = \gamma = 1$, with solitary wave initial conditions as taken in (73) with $p = 1$ to provide a significant non-zero mean value. The energy and momentum relations are plotted in Figure 11, where we note that the left-hand side of the mass equation (88) is equal to zero to machine precision and therefore is omitted from the plot.

We see that the derivatives of the energy and momentum oscillate with period $f = 2\pi/\omega$ between two different values. To verify the conservation laws, the peaks and troughs were tracked for both the left-hand side and right-hand side of the conservation laws and the absolute percentage error between peaks or troughs was calculated as $4.24 \times 10^{-6}\%$ for the energy and $3.60 \times 10^{-10}\%$ for the momentum. It is of note that

the left-hand side of these laws require a time derivative on discrete data and so the accuracy to which they are conserved is hampered by this limitation. In our case the time step was taken as $\Delta t = 0.001$.

VI. CONCLUSIONS

In this paper we developed an asymptotic procedure for the construction of the weakly-nonlinear solution of the Cauchy problem for a system of coupled regularised Boussinesq equations in the high-contrast case when the characteristic speeds in the layers are not close (i.e. the materials of the layers have essentially different elastic properties). Importantly, we removed the need to restrict the initial conditions only to functions with zero mean. The constructed solution was compared to the case when the characteristic speeds in the equations are close (low-contrast case).

We examined the accuracy of the constructed solution numerically, using direct numerical simulations for the coupled Boussinesq equations and our constructed semi-analytical so-

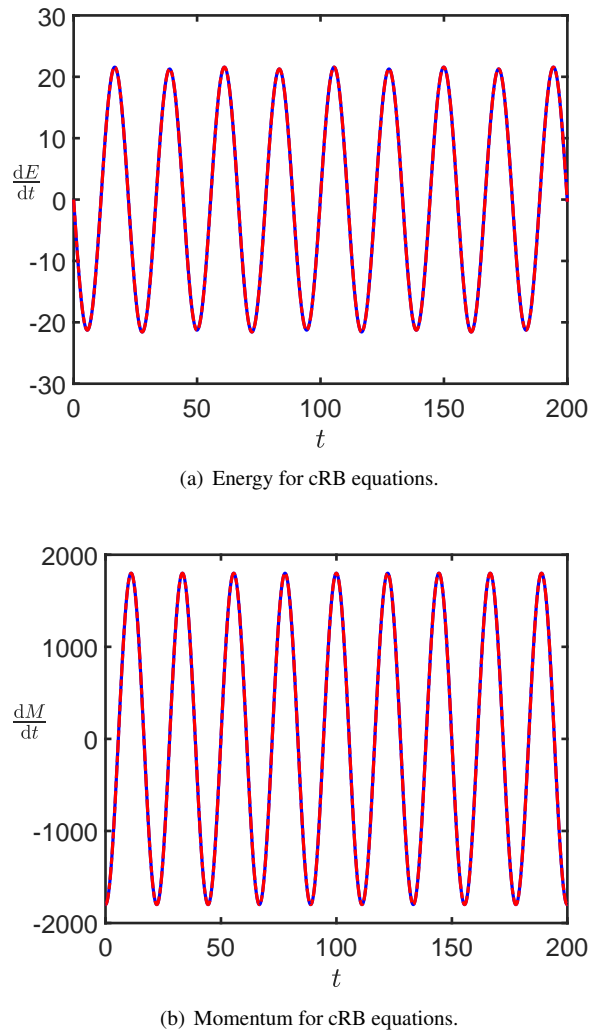


FIG. 11. Verification of the generalised conservation laws in the cRB equations, where the blue, solid line is the left-hand side of the relation and the red, dashed line is the right-hand side of the relation, for (a) energy and (b) momentum. Parameters are $L = 300$, $N = 60000$, $c = 1.025$, $\varepsilon = 0.01$, $\alpha = \beta = \delta = \gamma = 1$, $k_1 = k_2 = 1/\sqrt{2}$, $\Delta t = 0.001$ and $\Delta T = \varepsilon \Delta t$.

lution, and showed that the constructed solution is a good approximation to the direct numerical simulations, with improving accuracy for the inclusion of additional terms. In particular, we found that the inclusion of terms at $O(\sqrt{\varepsilon})$ allows us to take account of the mass with no need for solving additional equations to those at leading order.

We then studied the case of counter-propagating waves within the context of close or distinct characteristic speeds, for solitary wave initial conditions. We showed that radiating solitary waves or wave packets interact almost elastically and their structure appears qualitatively unchanged. Comparison to the case without interaction showed a minor change in amplitude and phase shift for radiating solitary waves, with a more distinct change for the wave packets, suggesting the

latter collisions are strongly inelastic.

Next we studied the behaviour of a cnoidal wave initial condition, and solutions for the high-contrast case were compared to that in the low-contrast case. For close characteristic speeds we see that radiating solitary waves are generated from each cnoidal wave peak. The tails interact with the preceding peak, so phase shift and amplitude changes occur in the tail. The amplitude of the main peak is changed by the interactions, however there is no significant phase shift introduced by the interactions. For distinct characteristic speeds, wave packets are generated by each peak, and we can clearly see the evolution of each peak into a wave packet, joined to its neighbours. The individual identities of the wave packets become harder to detect when the wavelength of the cnoidal wave is reduced - the radiation emitted by each wave packet is quickly absorbed by the next one, resulting in a more complicated periodic wave structure.

Finally, we showed that generalised conservation laws can be derived to take account of an initial condition that is not necessarily zero-mean. These conservation laws consist of one local (mass) and two non-local (energy and momentum) relations, with the conserved quantity oscillating with a frequency determined by the evolution of non-zero mass of the initial data, confirmed by numerical simulations. These non-local conservation laws are applicable when the waves propagate on the background of some initially pre-strained basic state characterised by non-zero mass of u and w .

The constructed solution can find useful applications in the studies of the scattering of radiating solitary waves by delamination,^{11,24} where the previous considerations were restricted to the initial conditions with either small or zero mean value because of the zero-mass contradiction. The propagation of cnoidal waves and undular bores^{25,26} in structures with defects is an interesting area for future research.

SUPPLEMENTARY MATERIALS

See supplementary material for Appendices A, B, and C, containing details of the numerical techniques used in this paper.

ACKNOWLEDGEMENTS

MRT is grateful to the UK QJMAM Fund for Applied Mathematics for the support of his travel to the ICoNSoM 2019 conference in Rome, Italy, where the initial discussions of this work have taken place. KRK is grateful to the organisers of the Dispersive Hydrodynamics research semester at the Isaac Newton Institute (INI) in the summer of 2022 for the invitation to participate in the program. The work was completed during her stay in Cambridge with the INI support under EPSRC grant number EP/R014604/1.

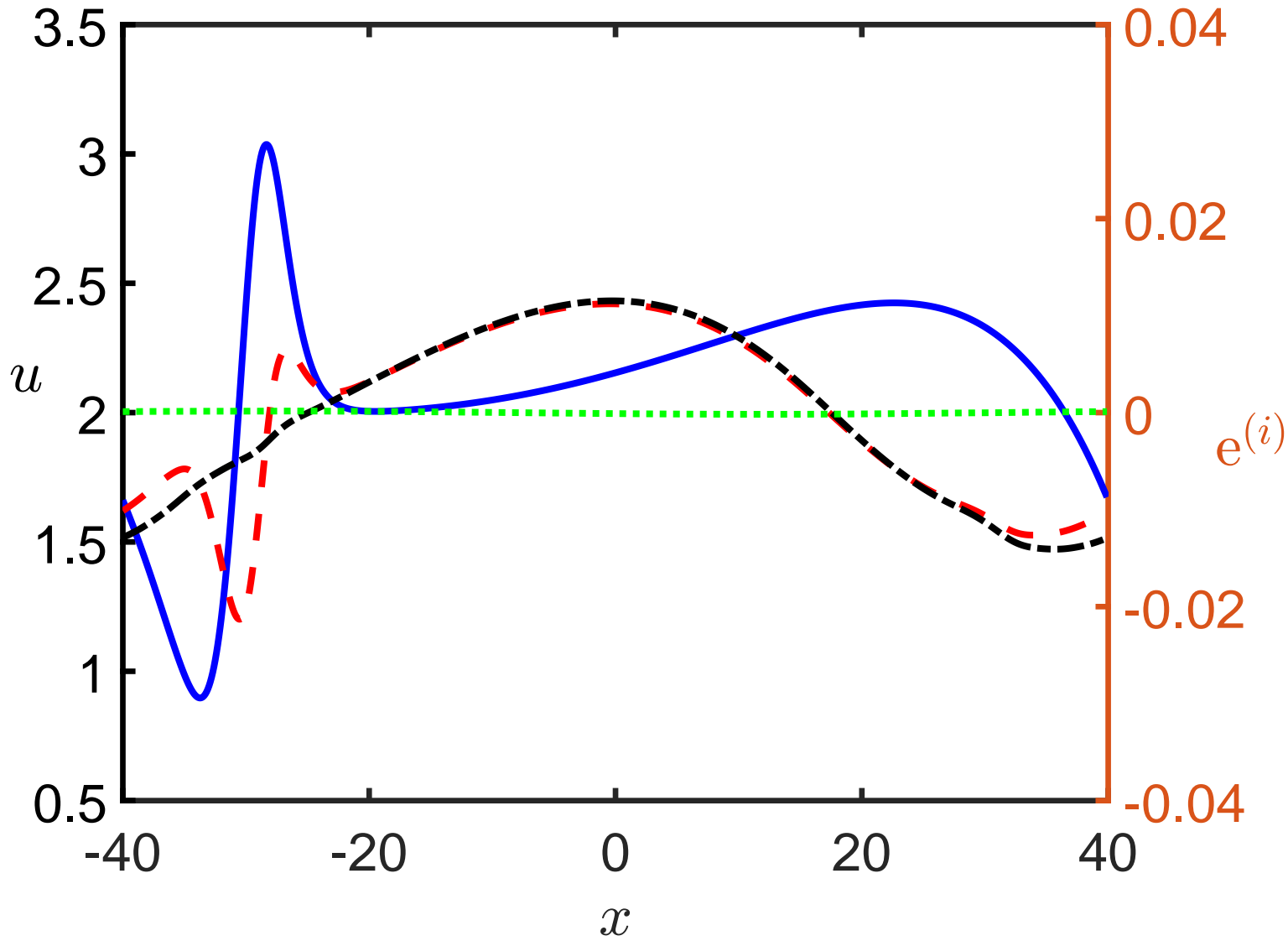
DATA AVAILABILITY STATEMENT

The data that support the findings of this study can be reproduced using the numerical schemes presented in the Supplementary Materials to the article. They are also available from the corresponding author upon reasonable request.

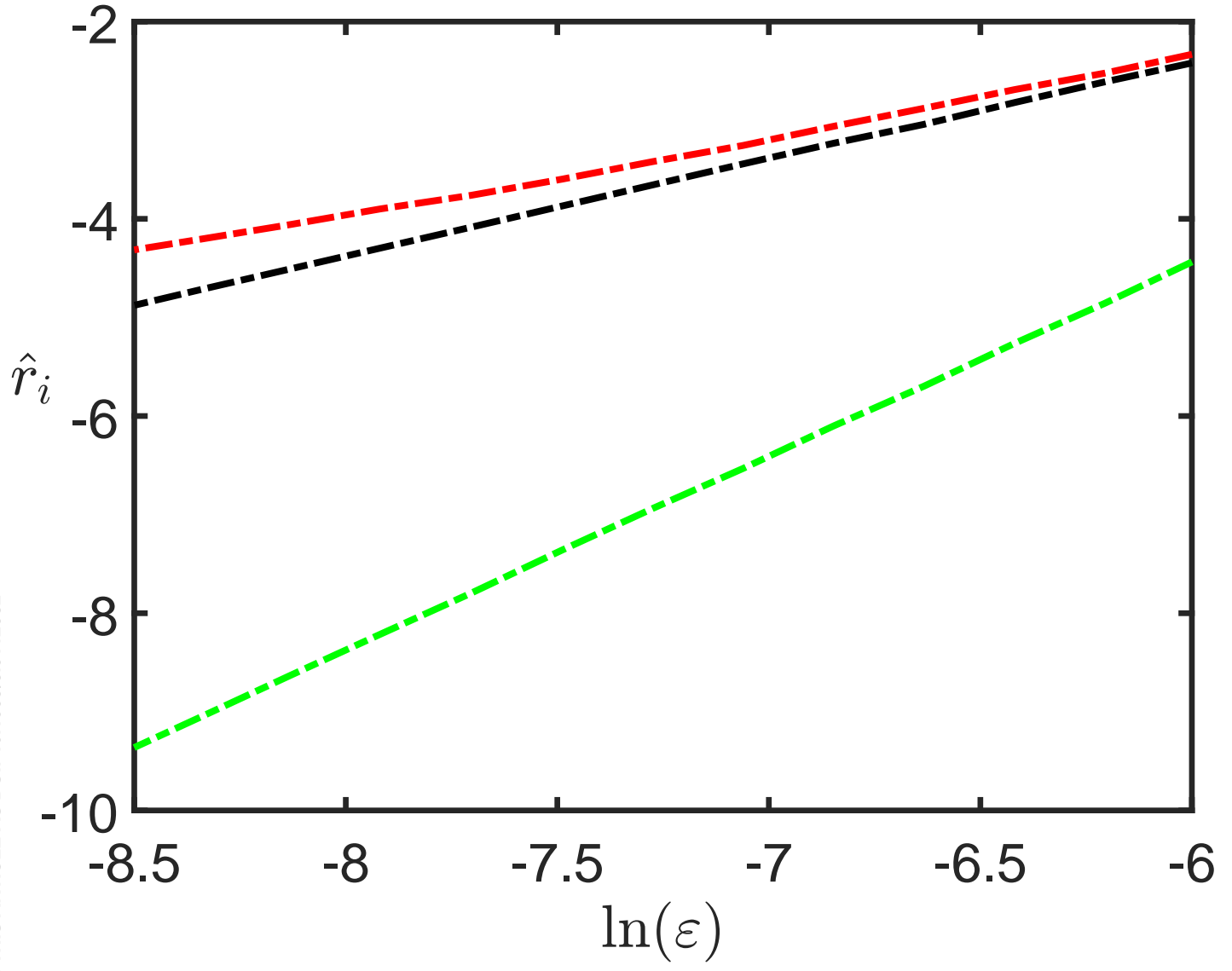
REFERENCES

- ¹G. A. Nariboli and A. Sedov, "Burgers's-Korteweg-De Vries equation for viscoelastic rods and plates," *J. Math. Anal. Appl.* **32**, 661–677 (1970).
- ²L. A. Ostrovsky and A. M. Sutin, "Nonlinear elastic waves in rods," *PMM* **41**, 531–537 (1977).
- ³A. M. Samsonov, *Strain Solitons in Solids and How to Construct Them* (Chapman & Hall/CRC, Boca Raton, 2001).
- ⁴A. V. Porubov, *Amplification of Nonlinear Strain Waves in Solids* (World Scientific, Singapore, 2003).
- ⁵V. I. Erofeev, V. V. Kazhaev, and N. P. Semerikova, *Waves in rods: dispersion, dissipation, nonlinearity* (Fizmatlit, Moscow, 2002).
- ⁶H.-H. Dai and X. Fan, "Asymptotically approximate model equations for weakly nonlinear long waves in compressible elastic rods and their comparisons with other simplified model equations," *Math. Mech. Solids* **9**, 61–79 (2004).
- ⁷T. Peets, K. Tamm, and J. Engelbrecht, "On the role of nonlinearities in the Boussinesq-type wave equations," *Wave Motion* **71**, 113–119 (2017).
- ⁸F. E. Garbuzov, K. R. Khusnutdinova, and I. V. Semenova, "On Boussinesq-type models for long longitudinal waves in elastic rods," *Wave Motion* **88**, 129–143 (2019).
- ⁹F. E. Garbuzov, Y. M. Beltukov, and K. R. Khusnutdinova, "Longitudinal bulk strain solitons in a hyperelastic rod with quadratic and cubic nonlinearities," *Theor. Math. Phys.* **202**, 319–333 (2020).
- ¹⁰K. R. Khusnutdinova, A. M. Samsonov, and A. S. Zakharov, "Nonlinear layered lattice model and generalized solitary waves in imperfectly bonded structures," *Phys. Rev. E* **79**, 056606 (2009).
- ¹¹K. R. Khusnutdinova and M. R. Tranter, "On radiating solitary waves in bi-layers with delamination and coupled Ostrovsky equations," *Chaos* **27**, 013112 (2017).
- ¹²K. R. Khusnutdinova, K. R. Moore, and D. E. Pelinovsky, "Validity of the weakly nonlinear solution of the Cauchy problem for the Boussinesq-type equation," *Stud. Appl. Math.* **133**, 52–83 (2014).
- ¹³K. R. Khusnutdinova and M. R. Tranter, "D'Alembert-type solution of the Cauchy problem for the Boussinesq-Klein-Gordon equation," *Stud. Appl. Math.* **142**, 551–585 (2019).
- ¹⁴L. A. Ostrovsky, "Nonlinear internal waves in a rotating ocean," *Oceanology* **18**, 119–125 (1978).
- ¹⁵R. H. J. Grimshaw, L. A. Ostrovsky, V. I. Shrira, and Y. A. Stepanyants, "Long nonlinear surface and internal gravity waves in a rotating ocean," *Surv. Geophys.* **19**, 289–338 (1998).
- ¹⁶E. S. Benilov, "On the surface waves in a shallow channel with an uneven bottom," *Stud. Appl. Math.* **87**, 1–14 (1992).
- ¹⁷Y. A. Stepanyants, "Nonlinear waves in a rotating ocean (the Ostrovsky equation and its generalizations and applications)," *Izv. Atmos. Ocean. Phys.* **56**, 16–32 (2020).
- ¹⁸K. R. Khusnutdinova and K. R. Moore, "Initial-value problem for coupled Boussinesq equations and a hierarchy of Ostrovsky equations," *Wave Motion* **48**, 738–752 (2011).
- ¹⁹R. H. J. Grimshaw, K. R. Khusnutdinova, and K. R. Moore, "Radiating solitary waves in coupled Boussinesq equations," *IMA J. Appl. Math.* **82**, 802–820 (2017).
- ²⁰K. R. Khusnutdinova and M. R. Tranter, "Weakly-nonlinear solution of coupled Boussinesq equations and radiating solitary waves," in *Dynamical Processes in Generalized Continua and Structures*, edited by H. Altenbach, A. Belyaev, V. Eremeyev, A. Krivtsov, and A. Porubov (Springer, 2019) Chap. 18, pp. 321–343.
- ²¹L. N. Trefethen, *Spectral Methods in MATLAB* (SIAM, Philadelphia, 2000).
- ²²K. van der Sande, G. A. El, and M. A. Hoefer, "Dynamic soliton - mean flow interaction with non-convex flux," *J. Fluid Mech.* **928**, A21 (2021).
- ²³M. Gioriti, T. Grava, R. Jenkins, K. T.-R. McLaughlin, and A. Minakov, "Solitons versus the gas: Fredholm determinants, analysis, and the rapid oscillations behind the kinetic equation," arXiv:2205.02601v3 [math-ph] (2022).
- ²⁴J. S. Tamber and M. R. Tranter, "Scattering of an Ostrovsky wave packet in a delaminated waveguide," *Wave Motion* , 103023 (2022).
- ²⁵C. G. Hooper, P. D. Ruiz, J. M. Huntley, and K. R. Khusnutdinova, "Undular bores generated by fracture," *Phys. Rev. E* **104**, 044207 (2021).
- ²⁶C. G. Hooper, K. R. Khusnutdinova, J. M. Huntley, and P. D. Ruiz, "Theoretical estimates of the parameters of longitudinal undular bores in PMMA bars based on their measured initial speeds," *Proc. Roy. Soc. A* (2022).

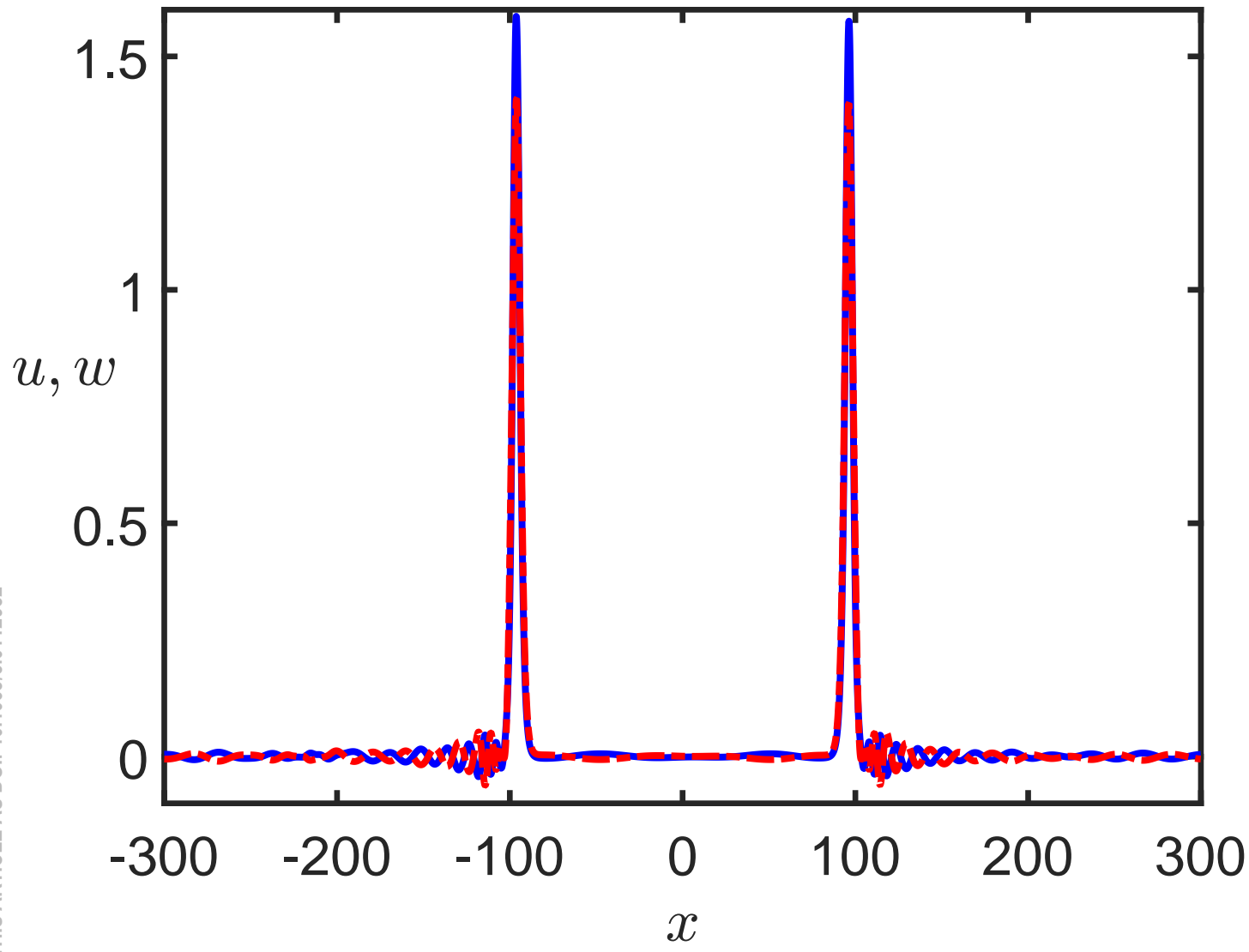
This is the author's peer reviewed, accepted manuscript. However, the online version of record will be different from this version once it has been copyedited and typeset.
PLEASE CITE THIS ARTICLE AS DOI: 10.1063/5.0112982



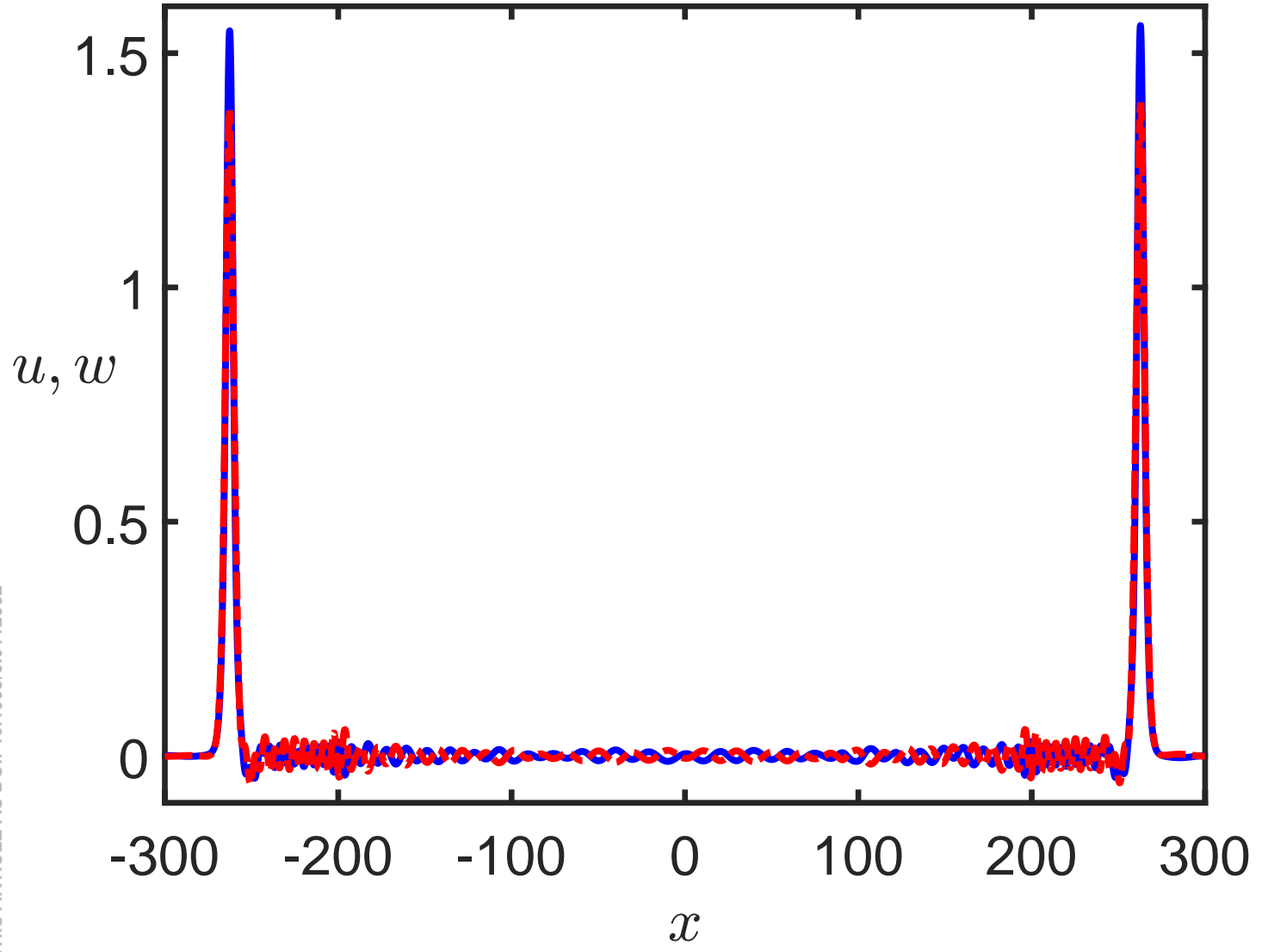
This is the author's peer reviewed, accepted manuscript. However, the online version of record will be different from this version once it has been copyedited and typeset.
PLEASE CITE THIS ARTICLE AS DOI: 10.1063/5.0112982



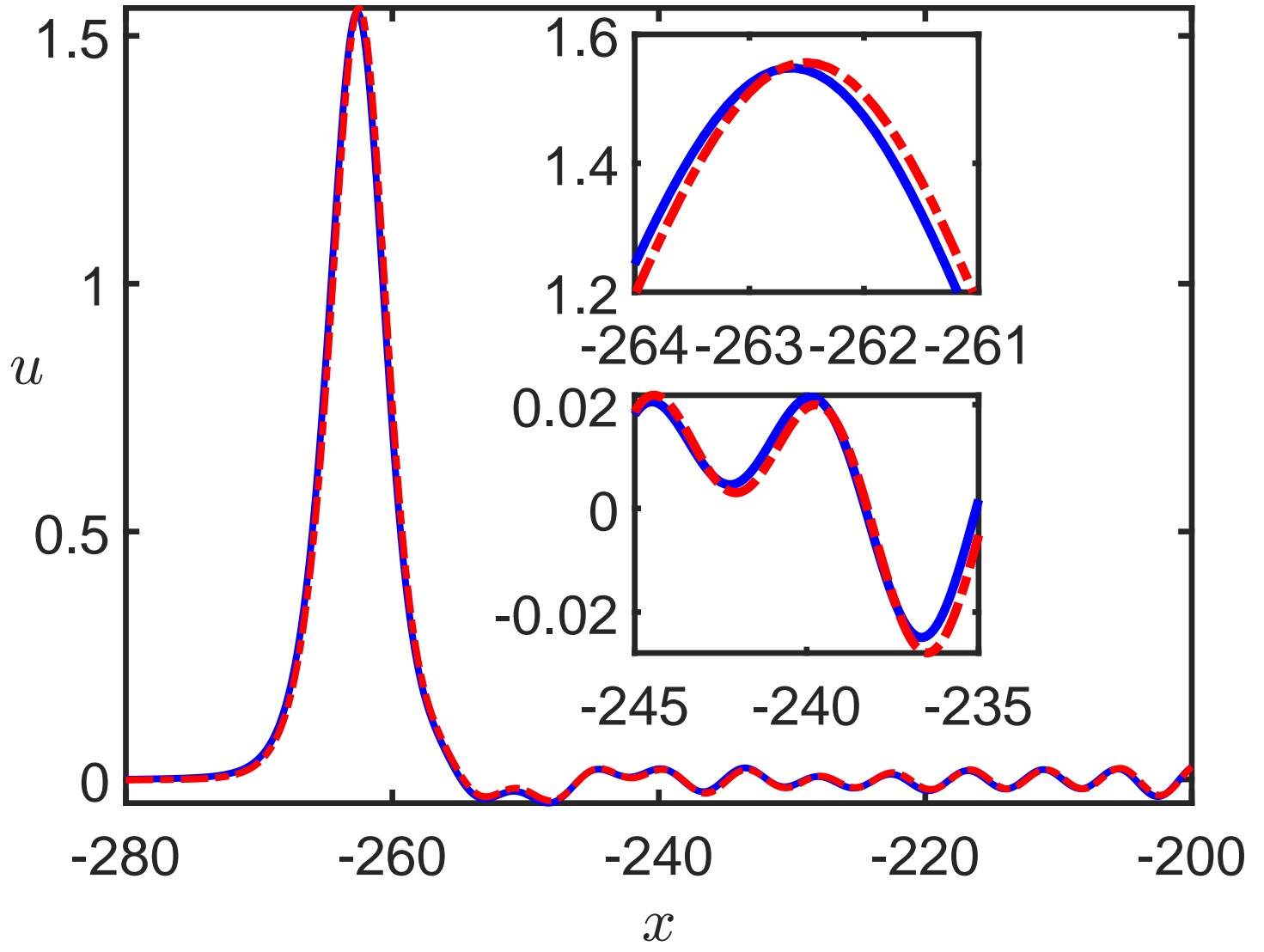
This is the author's peer reviewed, accepted manuscript. However, the online version of record will be different from this version once it has been copyedited and typeset.
PLEASE CITE THIS ARTICLE AS DOI: 10.1063/5.0112982



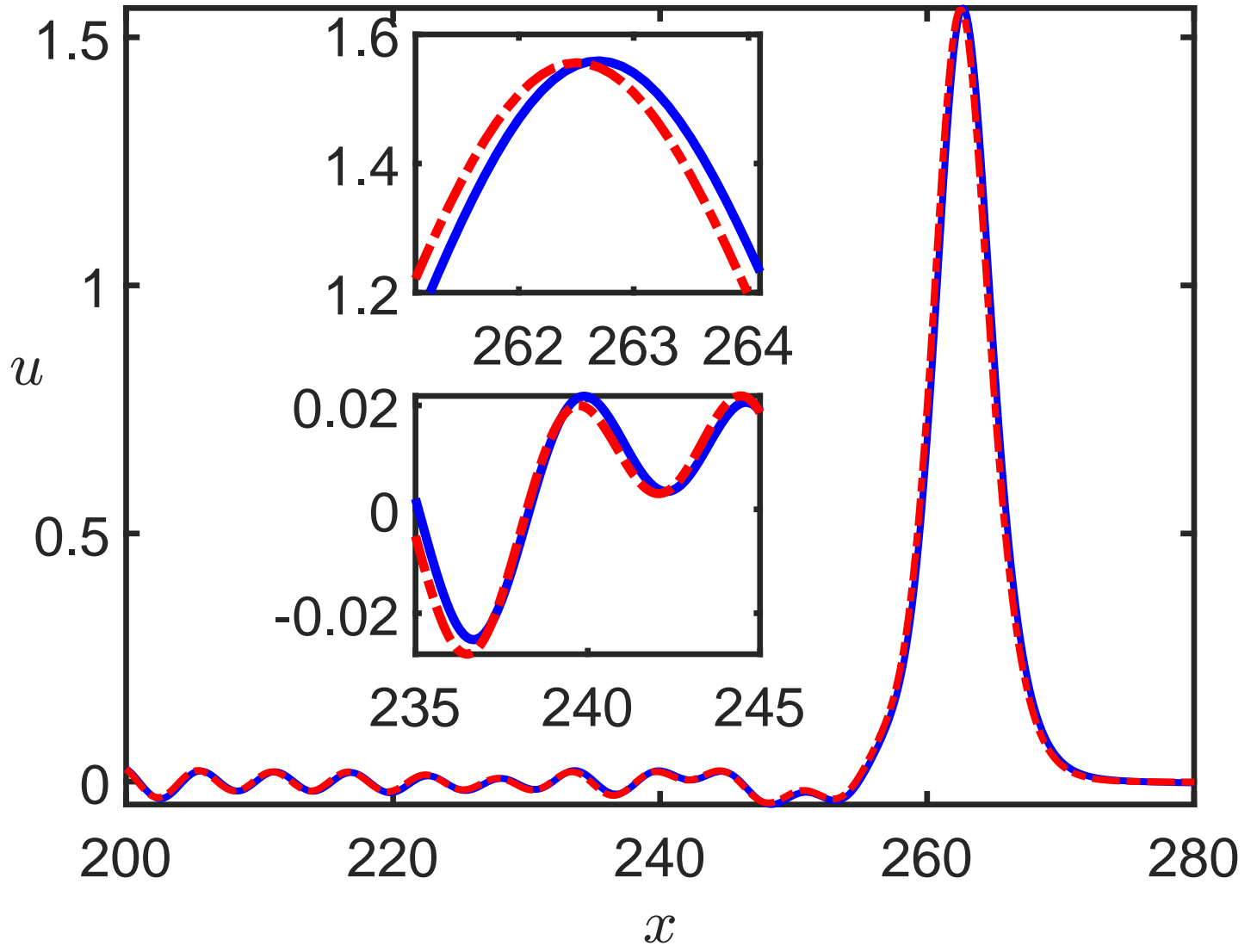
This is the author's peer reviewed, accepted manuscript. However, the online version of record will be different from this version once it has been copyedited and typeset.
PLEASE CITE THIS ARTICLE AS DOI: 10.1063/5.0112982



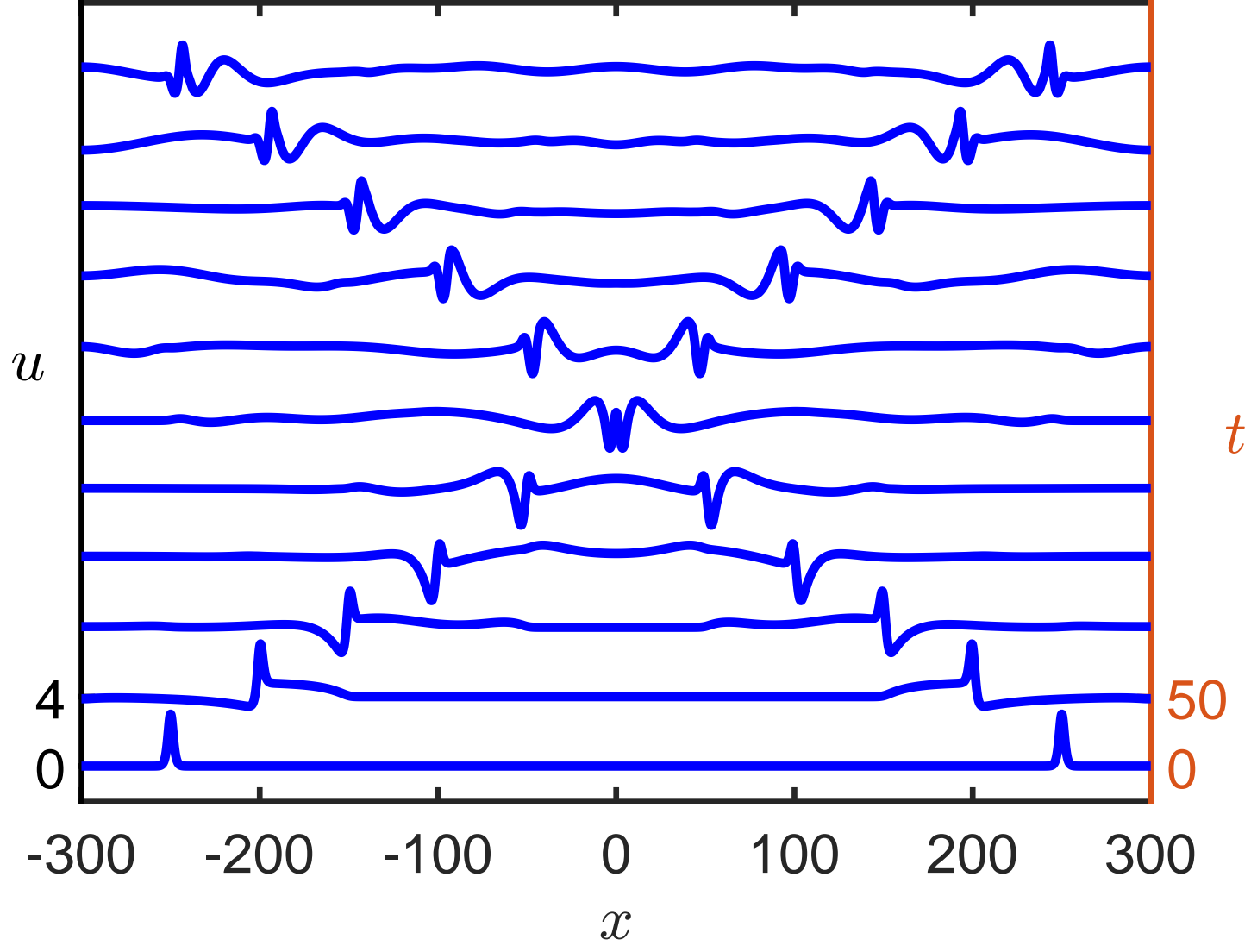
This is the author's peer reviewed, accepted manuscript. However, the online version of record will be different from this version once it has been copyedited and typeset.
PLEASE CITE THIS ARTICLE AS DOI: 10.1063/5.0112982



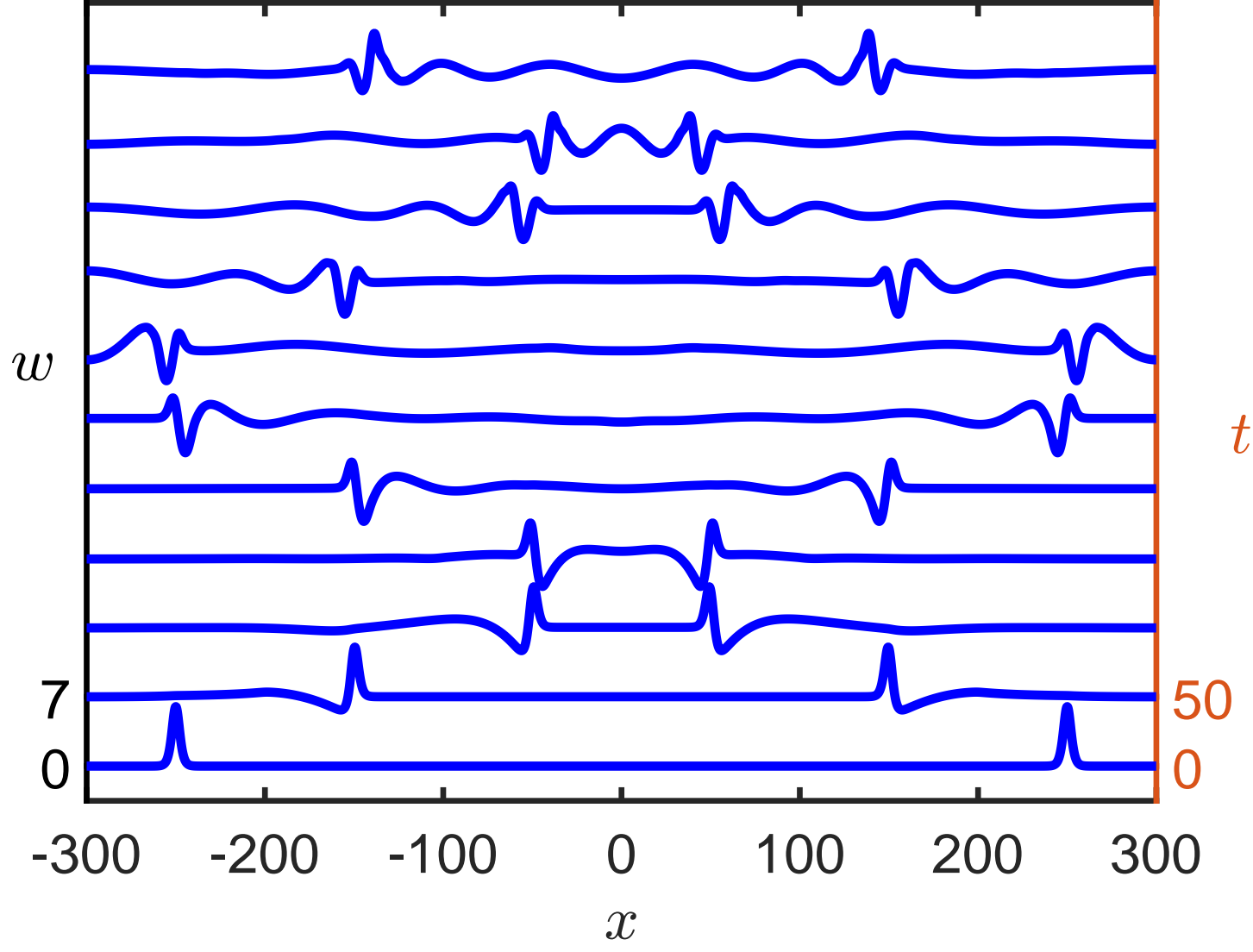
This is the author's peer reviewed, accepted manuscript. However, the online version of record will be different from this version once it has been copyedited and typeset.
PLEASE CITE THIS ARTICLE AS DOI: 10.1063/5.0112982



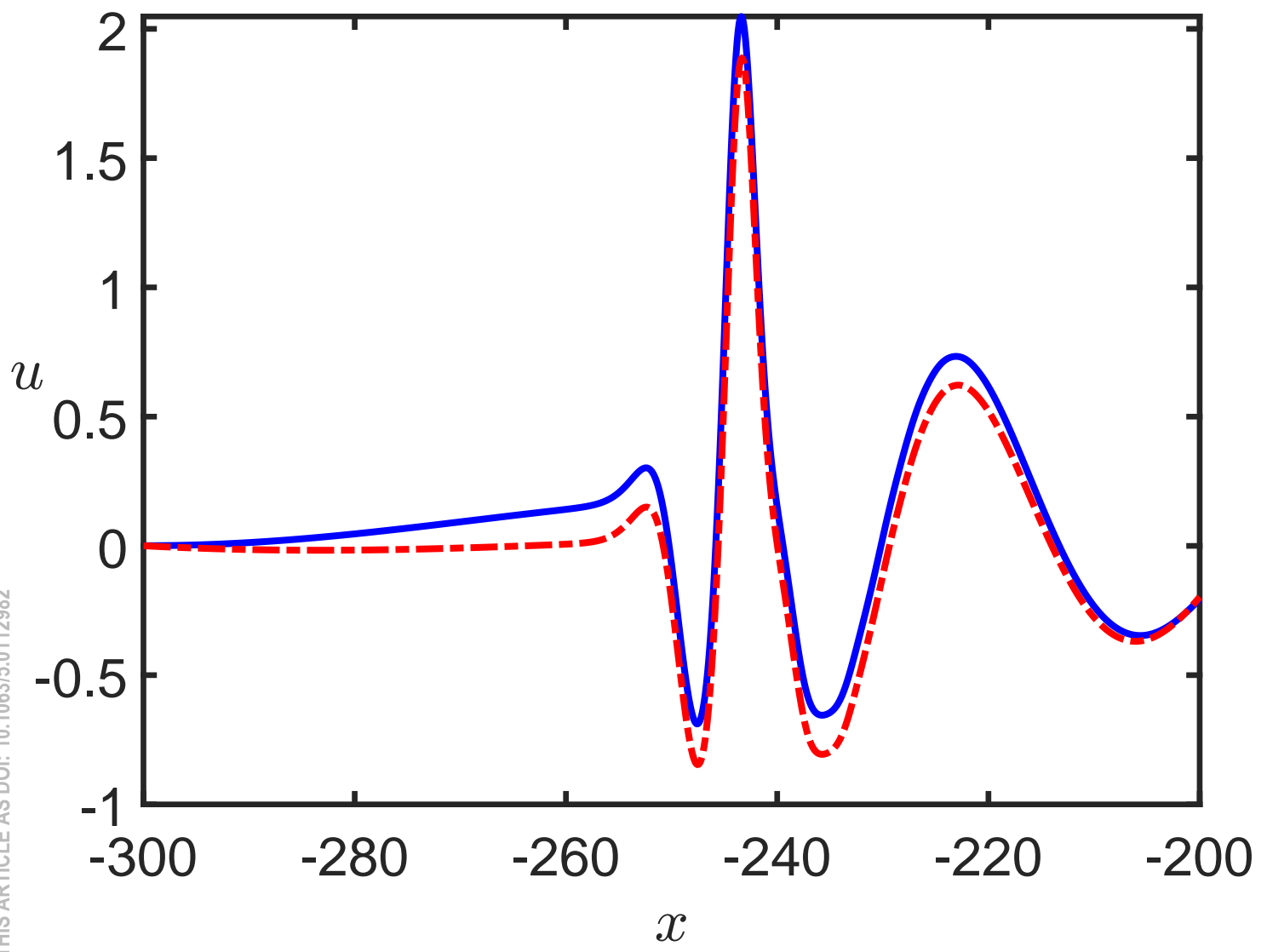
This is the author's peer reviewed, accepted manuscript. However, the online version of record will be different from this version once it has been copyedited and typeset.
PLEASE CITE THIS ARTICLE AS DOI: 10.1063/5.0112982



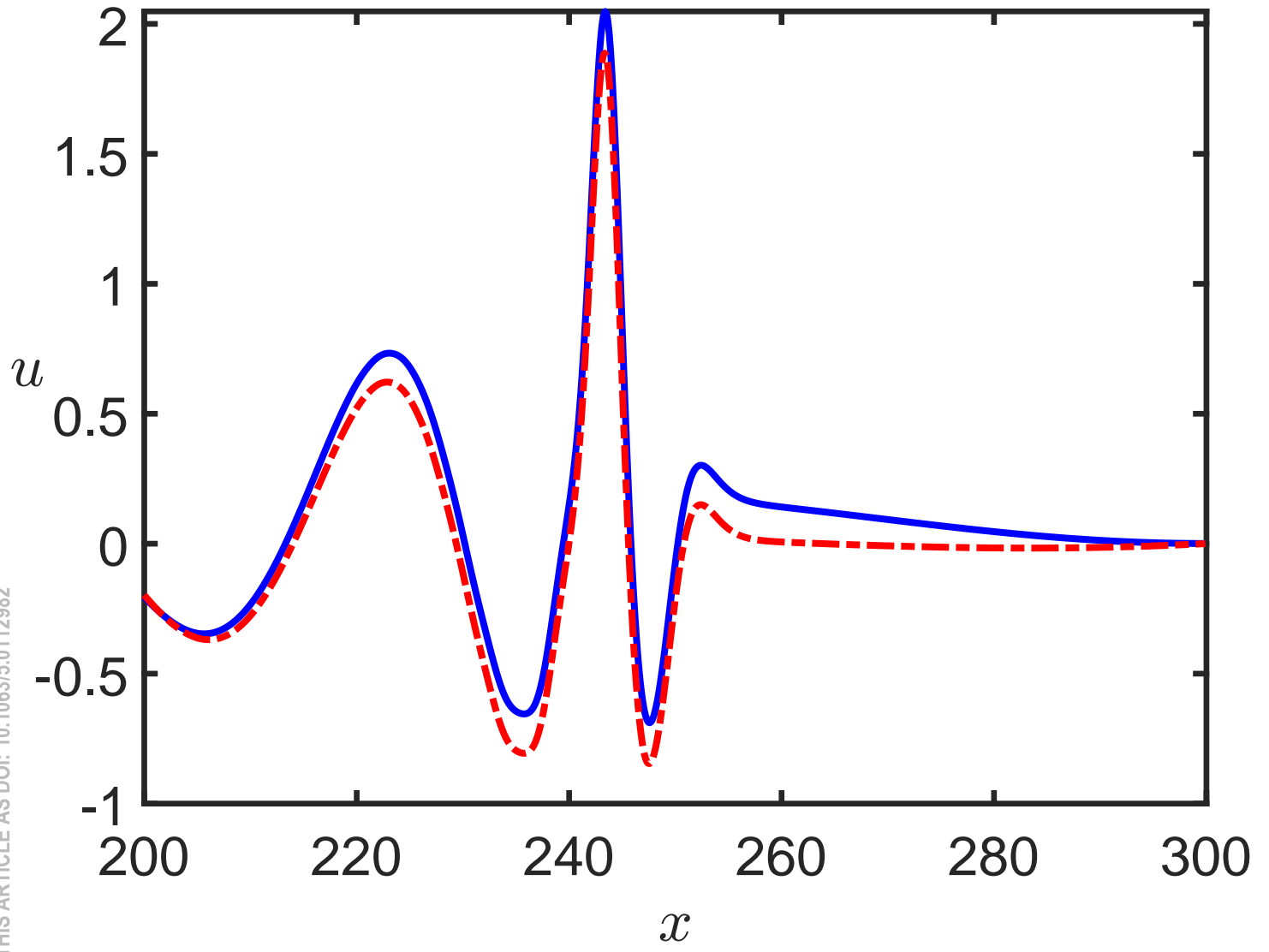
This is the author's peer reviewed, accepted manuscript. However, the online version of record will be different from this version once it has been copyedited and typeset.
PLEASE CITE THIS ARTICLE AS DOI: 10.1063/5.0112982



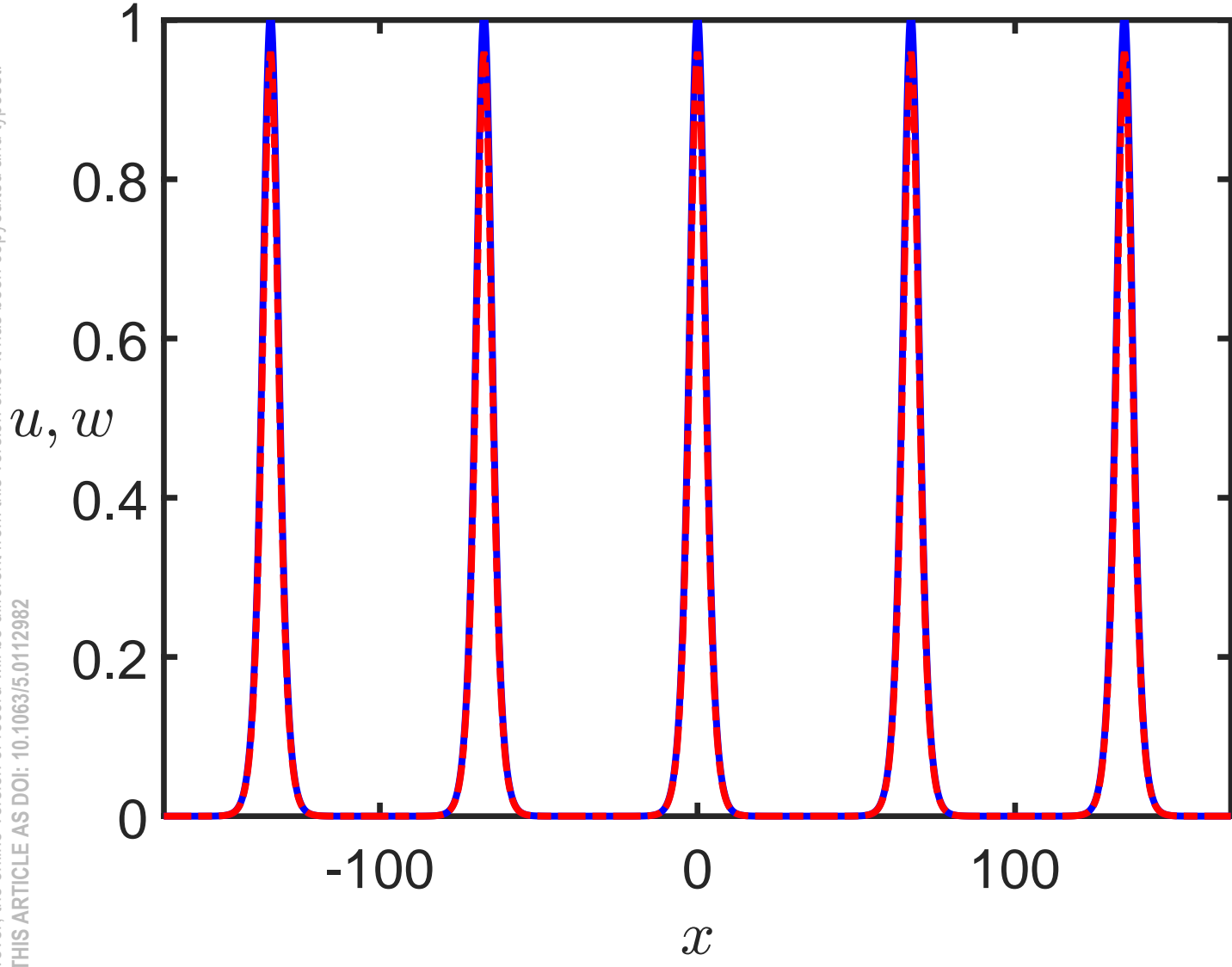
This is the author's peer reviewed, accepted manuscript. However, the online version of record will be different from this version once it has been copyedited and typeset.
PLEASE CITE THIS ARTICLE AS DOI: 10.1063/5.0112982



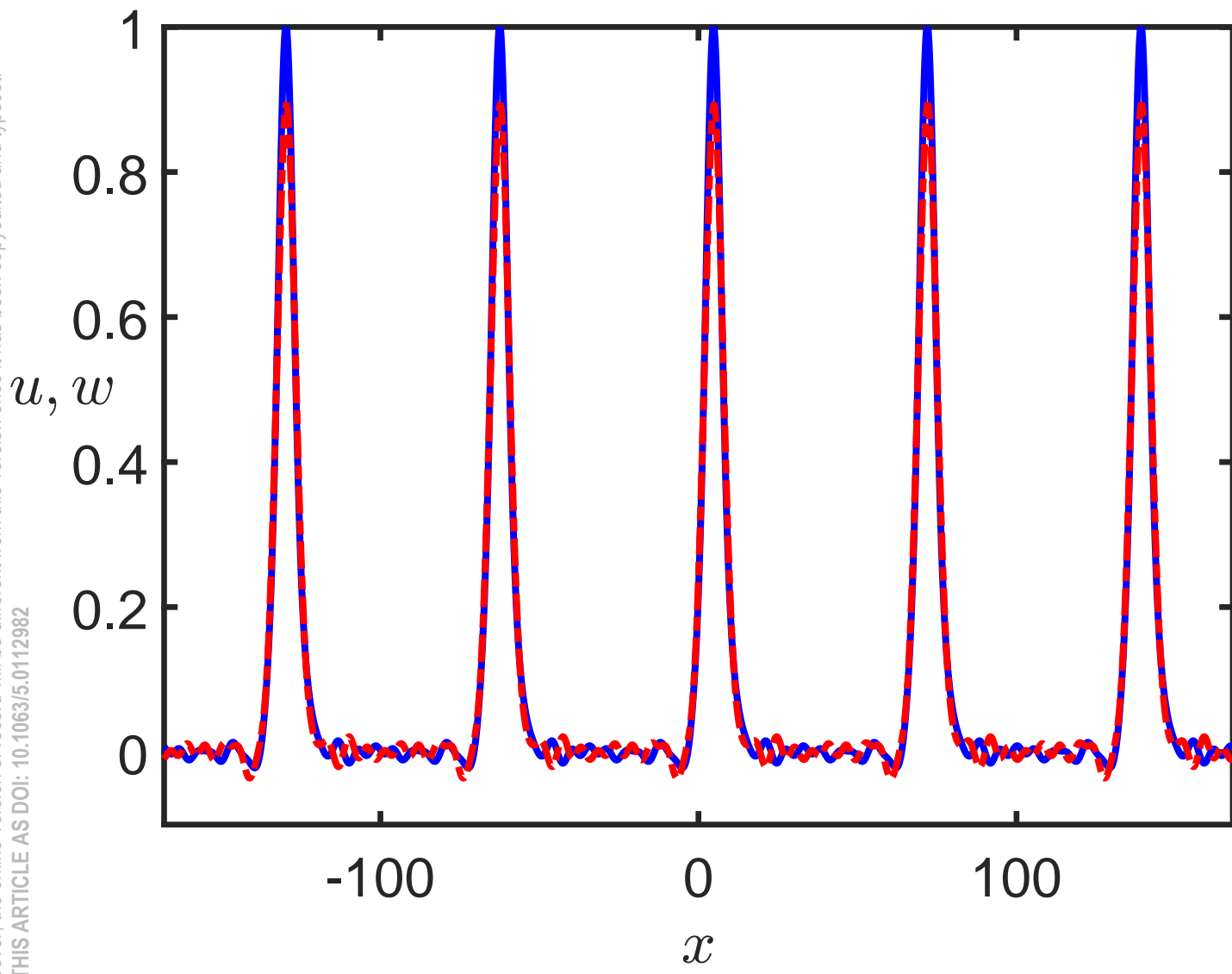
This is the author's peer reviewed, accepted manuscript. However, the online version of record will be different from this version once it has been copyedited and typeset.
PLEASE CITE THIS ARTICLE AS DOI: 10.1063/5.0112982



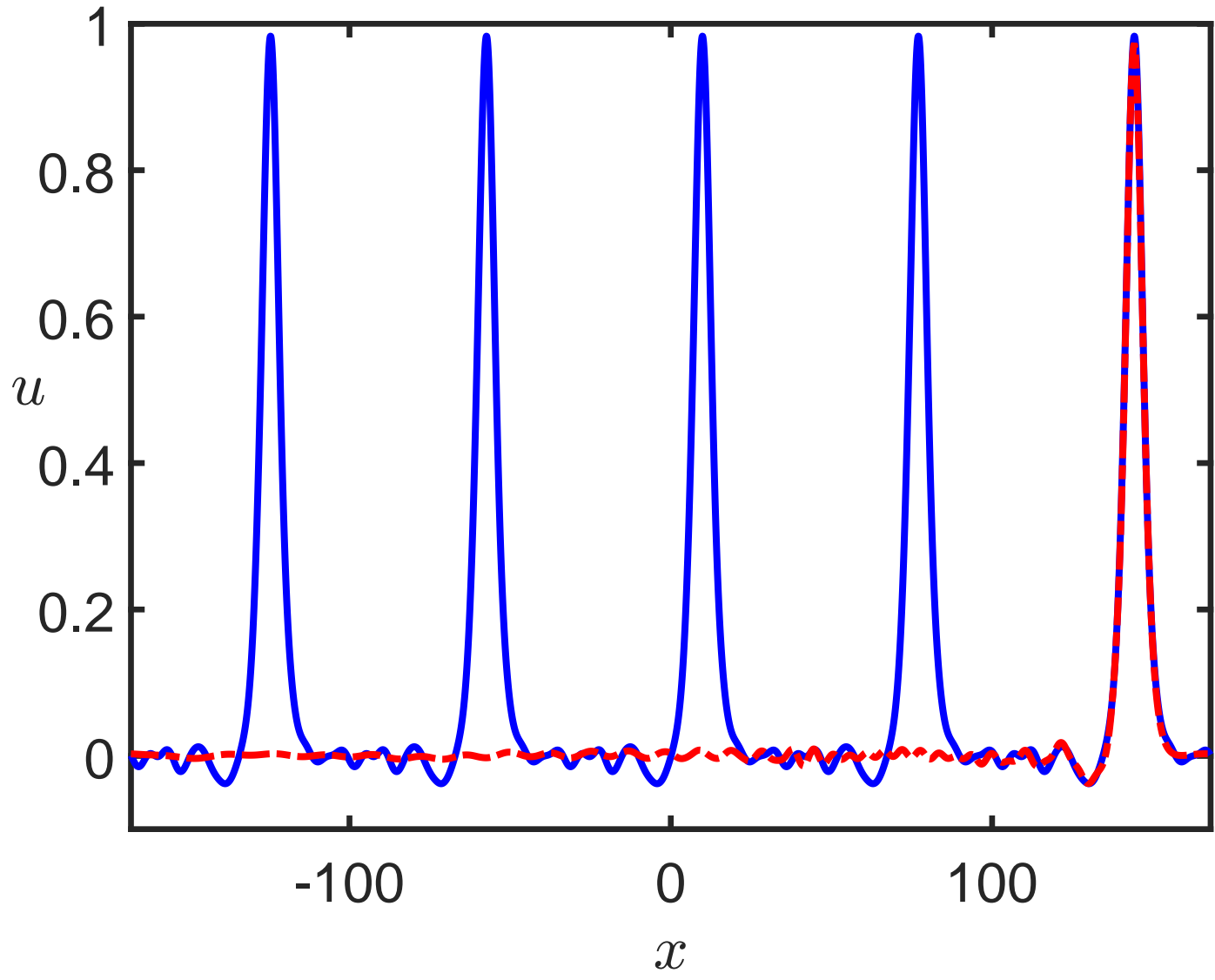
This is the author's peer reviewed, accepted manuscript. However, the online version of record will be different from this version once it has been copyedited and typeset.
PLEASE CITE THIS ARTICLE AS DOI: 10.1063/5.0112982



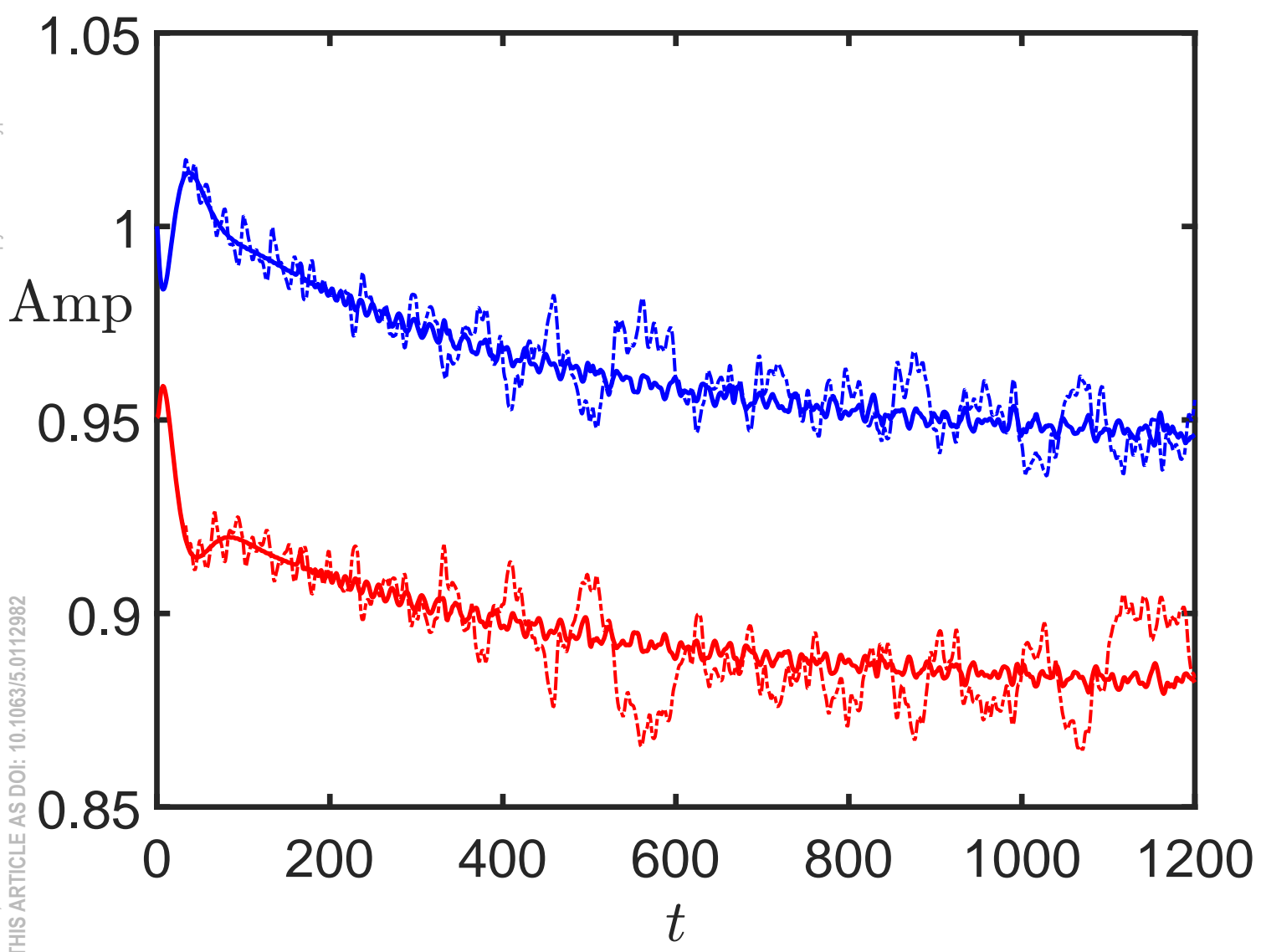
This is the author's peer reviewed, accepted manuscript. However, the online version of record will be different from this version once it has been copyedited and typeset.
PLEASE CITE THIS ARTICLE AS DOI: 10.1063/5.0112982



This is the author's peer reviewed, accepted manuscript. However, the online version of record will be different from this version once it has been copyedited and typeset.
PLEASE CITE THIS ARTICLE AS DOI: 10.1063/5.0112982

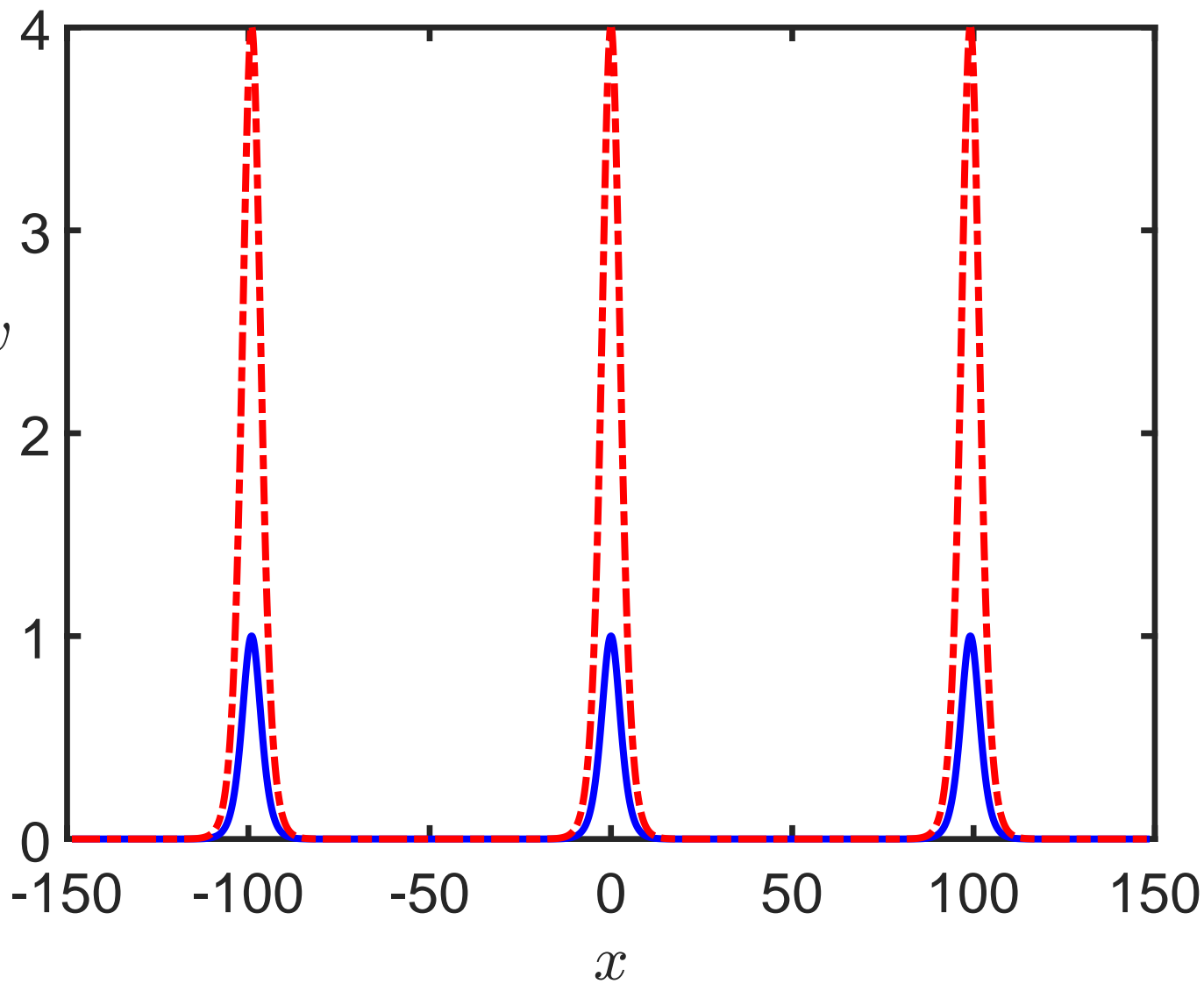


This is the author's peer reviewed, accepted manuscript. However, the online version of record will be different from this version once it has been copyedited and typeset.
PLEASE CITE THIS ARTICLE AS DOI: 10.1063/5.0112982



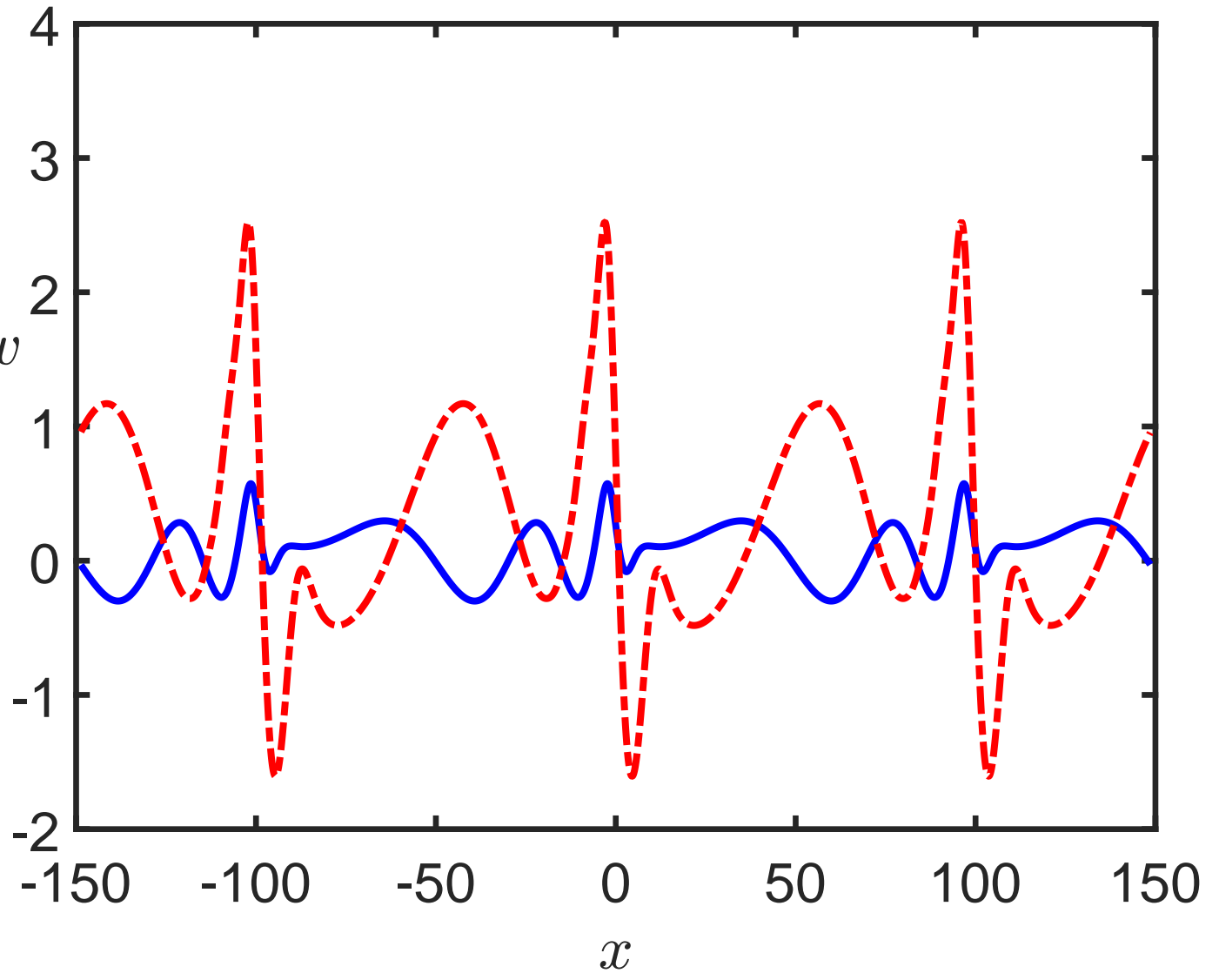
This is the author's peer reviewed, accepted manuscript. However, the online version of record will be different from this version once it has been copyedited and typeset.
PLEASE CITE THIS ARTICLE AS DOI: 10.1063/5.0112982

u, w

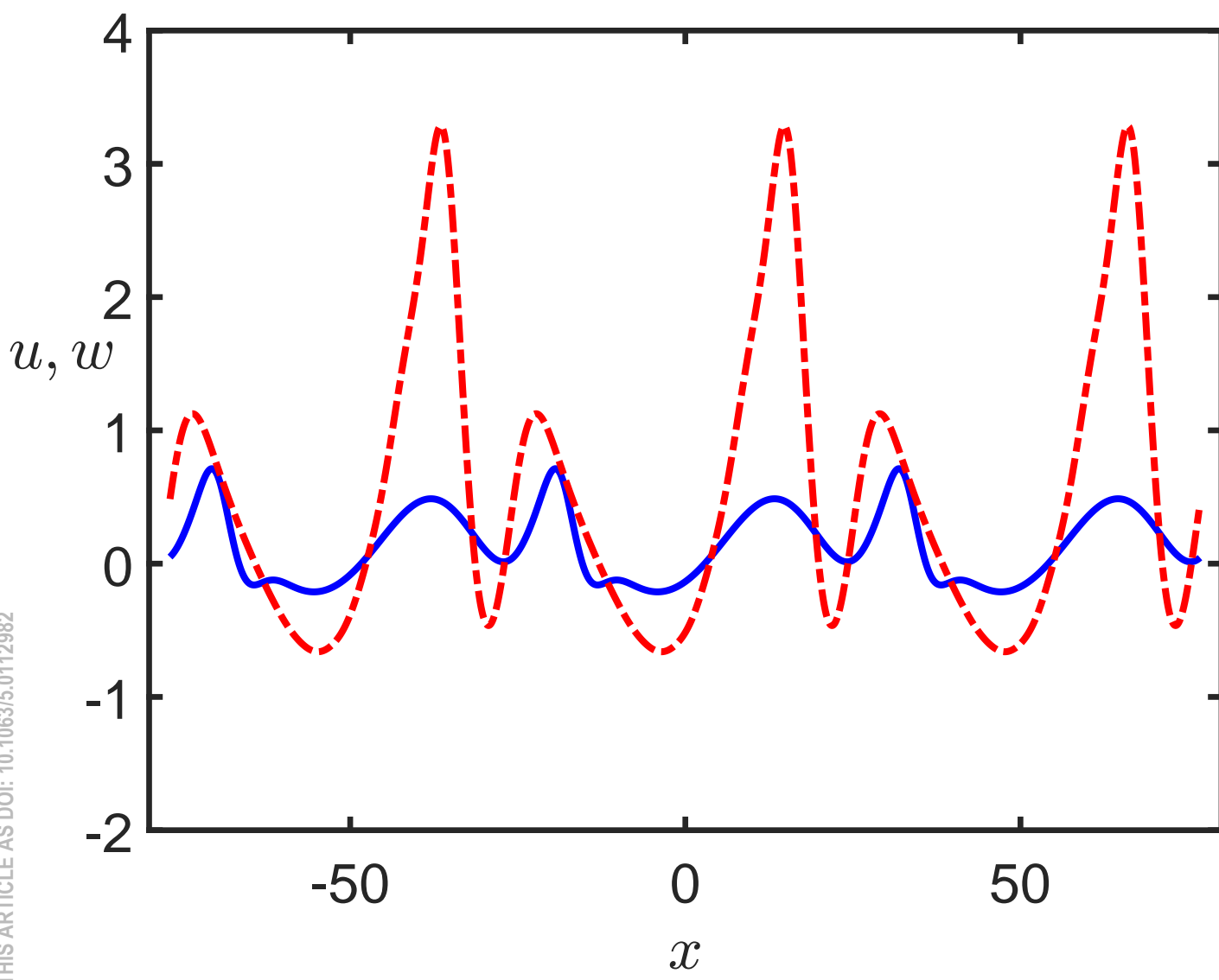


This is the author's peer reviewed, accepted manuscript. However, the online version of record will be different from this version once it has been copyedited and typeset.
PLEASE CITE THIS ARTICLE AS DOI: 10.1063/5.0112982

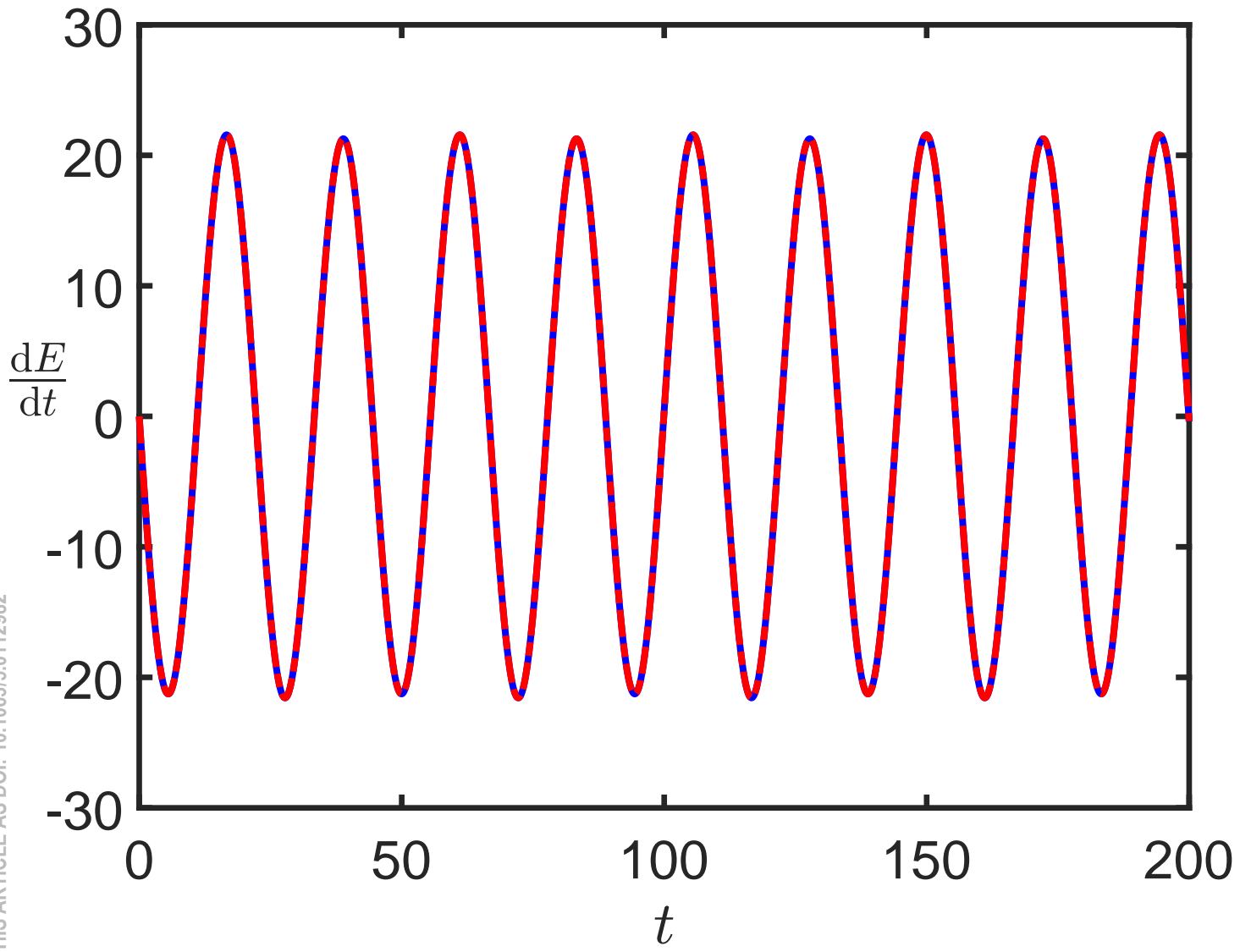
u, w



This is the author's peer reviewed, accepted manuscript. However, the online version of record will be different from this version once it has been copyedited and typeset.
PLEASE CITE THIS ARTICLE AS DOI: 10.1063/5.0112982



This is the author's peer reviewed, accepted manuscript. However, the online version of record will be different from this version once it has been copyedited and typeset.
PLEASE CITE THIS ARTICLE AS DOI: 10.1063/5.0112982



This is the author's peer reviewed, accepted manuscript. However, the online version of record will be different from this version once it has been copyedited and typeset.
PLEASE CITE THIS ARTICLE AS DOI: 10.1063/5.0112982

